Michigan Institute for Plasma Science and Engineering (MIPSE)

13th ANNUAL GRADUATE STUDENT SYMPOSIUM

November 16, 2022
University of Michigan North Campus, Ann Arbor, MI 48109

Schedule

I. Special MIPSE Seminar

3213 (Johnson Rooms), **Lurie Engineering Center**, 1221 Beal Avenue

12:30 – 12:55 pm	**Registration, refreshments**
12:55 – 1:00 pm	**Prof. Mark J. Kushner**, University of Michigan Director, MIPSE ***Opening remarks***
1:00 – 2:00 pm	Special MIPSE seminar **Dr. Radha Bahukutumbi,** Laboratory for Laser Energetics, Univ. of Rochester ***Unraveling Implosion Physics in Inertial Confinement Fusion: Direct-drive Simulations, Experiments, and Physics-informed Data Science***
2:00 – 2:15 pm	**Prof. Sergey Baryshev**, Michigan State University Chair, AVS Michigan Chapter ***Introducing American Vacuum Society Michigan Chapter***

II. Student Posters

Atrium, **EECS Building**, 1301 Beal Avenue

2:30 – 3:00 pm	Poster setup
3:00 – 3:50 pm	**Poster session I**
3:50 – 4:40 pm	**Poster session II**
4:40 – 5:30 pm	**Poster session III**
5:30 – 5:45 pm	Poster removal
5:45 – 6:00 pm	***Best Presentation Award* ceremony**

Participating institutions: University of Michigan, Michigan State University, University of Notre Dame, University of Toledo, SUNY Buffalo.

Poster Session I

1-01	**Qian Qian**	U-M	***Spin and Polarization-dependent Osiris QED Module for the Future Strong Field QED Laser-plasma Experiment***
1-02	**Ibukunoluwa Akintola**	Notre Dame	***Understanding Temperature Inhibition of Methane Conversion in DBD Plasma Using Electrical Characterization and Optical Emission Spectroscopy***
1-03	**Md Arifuzzaman Faisal**	MSU	***Grating Optimization for Smith-Purcell Radiation: Direct Correlation between Spatial Growth Rate and Starting Current***
1-04	**Salvatore Baldinucci**	U-M	***Model for Impact of Wall Material on ECR Magnetic Nozzle Operation***
1-05	**Gina Vasey**	MSU	***Identifying Governing ODEs in Irregular Physical Domain with Diffusion***
1-06	**Kelsey Williams**	SUNY Buffalo	***Development of a Microstrip Half-Wave Split-Ring Resonator for Microwave-Assisted Laser-Induced Breakdown Spectroscopy and Laser Ablation Molecular Isotopic Spectrometry***
1-07	**Thomas Marks**	U-M	***Correlations between Empirical and Self-consistent Anomalous Transport Models in Hall Thrusters***
1-08	**Julia Marshall**	U-M	***Resolving Extended Space and Time Correlations in Molecular Dynamics Simulations of Strongly Magnetized Plasmas***
1-09	**Sankhadeep Basu**	MSU	***Non-thermal Plasma Synthesis of Hydrophobic Silicon Nanoparticles***
1-10	**Michael Wadas**	U-M	***A Hydrodynamic Mechanism for Hot Spot Formation in the Remnant of SN1987A***
1-11	**Joshua Latham**	U-M	***Relativistic Laser Perturbation to Laser-Driven Magnetic Reconnection***
1-12	**Cameron Papson**	MSU	***Nonthermal Plasma Synthesis of Carbon Nanodots***
1-13	**Sandeep Narasapura Ramesh**	U. Toledo	***Frequency-Selective Plasma Limiters***
1-14	**Farha Islam Mime**	MSU	***Femtosecond Laser Formation of NV Centers in Diamond and STED Microscopy Characterization***
1-15	**Florian Krüger**	U-M	***Hybrid Optimization Method for Parameter Fitting in High Aspect Ratio Etching***
1-16	**Julian Kinney**	U-M	***Exploring the Importance of Temperature-Dependent Opacities in the Modeling of X-Ray Induced Thermomechanical Shock Experiments***

Poster Session II

2-01	**Ayush Paudel**	MSU	***A Discrete Cavity Analysis of Coupled-cavity Travelling Wave Tubes***
2-02	**André Antoine**	U-M	***Data-driven Modelling of Laser-plasma Experiments Enabled by Large Datasets***
2-03	**Zhongyu Cheng**	Notre Dame	***Non-thermal Plasma Jet Sintering of Indium Tin Oxide Thin Films***
2-04	**Kseniia Konina**	U-M	***Interaction of Atmospheric Pressure Plasma Jets with Complex Surfaces of Different Dielectrics***
2-05	**Taha Posos**	MSU	***Enabling Bright Carbon Nanotube Fiber Field Emission Cathode***
2-06	**Ryan Revolinsky**	U-M	***Design and Demonstration of a Dual Frequency, Harmonic, Magnetically Insulated Line Oscillator***
2-07	**Sarah Roberts**	MSU	***Microwave Plasma Assisted Chemical Vapor Deposition Process Variable Optimization of Nitrogen Doped Single Crystal Diamond***
2-08	**Michael Springstead**	U-M	***Developing a Shock-Ramp Laser Drive to Extend the Pressure Ranges of the NIF Gbar Platform Single-Shock Hugoniot Measurements***
2-09	**Kazi Kabir**	U. Toledo	***Evanescent-Mode Cavity Resonator-Based Microwave Plasma Jet Technology***
2-10	**Cristian Herrera-Rodriguez**	MSU	***MPACVD Diamond: Growth Conditions and Power Electronics Applications***
2-11	**Jordyn Polito**	U-M	***Reaction Mechanisms for Atmospheric Pressure Plasma Treatment of Organic Molecules in Solution***
2-12	**George Dowhan**	U-M	***Faraday Rotation Imaging of X-Pinch Implosion Dynamics***
2-13	**Christopher Sercel**	U-M	***Inductive Probing in a Rotating Magnetic Field Thruster***
2-14	**Khalil Bryant**	U-M	***Preliminary Results for Experiment at WiPPL***
2-15	**Donovan White**	U-M	***Beryllium Probe Neutron Diagnostic for a Gas-Puff Z-Pinch Neutron Source on a 1-MA, 100-ns Linear Transformer Driver***

Poster Session III

3-01	**Thomas Chuna**	MSU	***Conservative Structure Functions Via BGK Transport Equation***
3-02	**Garam Lee**	Notre Dame	***Investigation of the Interaction Between Non-Thermal Plasma Activated Nitrogen and Metal Surfaces***
3-03	**Leanne Su**	U-M	***Plasma Parameter Scaling at High Powers for a Magnetically Shielded Hall Thruster Operating on Krypton***
3-04	**Parker Roberts**	U-M	***Mitigation of Stray Light for Low-Temperature Thomson Scattering in DIII-D***
3-05	**Evan Litch**	U-M	***Low Bias Frequencies in ICP Reactors for High Aspect Ratio Plasma Etching***
3-06	**Andre Antoine**	U-M	***Characterizing Hot Electrons in Ensemble PIC Simulations of High-intensity, Laser-plasma Interactions with Machine Learning***
3-07	**Yang Zhou**	MSU	***Quantum Pathways Interference in Photoemission from Biased Metal Surfaces Induced by Two-color Lasers***
3-08	**Kwyntero Kelso**	U-M	***Photoionization Front Laboratory Experiments at the OMEGA Laser Facility***
3-09	**Nicholas Ernst**	U-M	***Controllable Electron Injection for Laser Wakefield Acceleration Using Co-Propagating Laser Pulses***
3-10	**Tanvi Nikhar**	MSU	***Evidence of Gas Phase Nucleation of Nano Diamond Through the Analysis of Activation Energy***
3-11	**Moises Angulo Enriquez**	U-M	***Numerical Simulation of the Hollow Cathode Plasma Discharge Using the Continuum-kinetic Method in 2D-2V***
3-12	**Joe Chen**	U-M	***Exploding Thin Liner Experiment on MAIZE***
3-13	**Dion Li**	U-M	***Induced Current Due to Electromagnetic Shock Produced by Charge Impact on a Conducting Surface***
3-14	**S M Asaduzzaman**	MSU	***Chemical Mechanical Polishing Rate and Surface Roughness for Single-Crystalline Diamond Substrates***
3-15	**Collin Whittaker**	U-M	***A Multi-Site Emission Modeling Framework for Porous Electrosprays***
3-16	**Madison Allen**	U-M	***Model Calibration using an Optimal Experimental Design for Ion Current Density and Ion Energy***

I-01. Spin and Polarization-dependent Osiris QED Module for the Future Strong Field QED Laser-plasma Experiment*

Q. Qian [a], D. Seipt [b,c], M. Vranic [d], T. Grismayer [d], T. Blackburn [e], C. P. Ridgers [f], A.G.R. Thomas [a]

(a) University of Michigan, Gérard Mourou Center of Ultrafast Optical Science, Ann Arbor, Michigan 48109-2099, USA (qqbruce@umich.edu)
(b) Helmholtz Institut Jena, Fröbelstieg 3, 07743 Jena, Germany
(c) GSI Helmholtzzentrum für Schwerionenforschung GmbH, Planckstrasse 1, 64291 Darmstadt, Germany
(d) GoLP/Instituto de Plasmas e Fusão Nuclear, Instituto Superior Técnico, Universidade de Lisboa, 1049-001 Lisbon, Portugal
(e) Department of Physics, University of Gothenburg, SE-41296 Gothenburg, Sweden
(f) York Plasma Institute, Department of Physics, University of York, York YO10 5DD, United Kingdom

With the rapid development of high-power petawatt class lasers worldwide, exploring the physics in the strong field QED regime will become one of the frontiers for laser-plasma interaction research. Particle-in-cell codes including quantum emission processes are powerful tools for predicting and analyzing future experiments, where the physics of relativistic plasma is strongly affected by strong-field QED processes. Here, we present the development of a full spin and polarization-included QED module based on the particle-in-cell code OSIRIS. In this module, the dynamics of the lepton's spin involve both the classical spin precession process described by the classical T-BMT equation and the quantum radiation reaction-induced spin transition process. The photon polarization-resolved quantum radiation rate allows us to assign the polarization state for each generated photon in the simulation. We also consider the influence of the lepton spin and photon polarization on the Non-linear Breit-Wheeler pair production process calculation. Compared with state-of-the-art, most common spin/polarization averaged QED modules, this full spin/polarization distinguished quantum module is able to more accurately simulate multi-staged processes like avalanche and shower type electron-positron pair production cascade processes. We also use this module to explore possible routines for generating polarized gamma-ray and lepton bunch through laser-plasma interaction.

*This work is supported by the NSF (Award No. 2108075).

I-02. Understanding Temperature Inhibition of Methane Conversion in DBD Plasma Using Electrical Characterization and Optical Emission Spectroscopy

Ibukunoluwa Akintola [a], Gerardo Rivera-Castro [b], Jason C. Hicks [b], and David B. Go [a, b]

(a) Department of Mechanical Engineering, University of Notre Dame (iakintol@nd.edu)
(b) Department of Chemical and Biomolecular Engineering, University of Notre Dame (dgo@nd.edu)

Non-thermal plasmas (NTPs) produce highly reactive chemical environments made up of electrons, ions, radicals, and vibrationally excited molecules. These reactive species, when combined with catalysts, can help drive thermodynamically unfavorable chemical reactions at low temperatures and atmospheric pressure. We are particularly interested in the direct coupling of light hydrocarbons (e.g., methane) and nitrogen to produce value-added liquid chemicals (e.g. pyrrole and pyridine) in a plasma-assisted catalytic process. To effectively create these plasma catalytic systems, a fundamental understanding of the plasma-phase chemistry alone is imperative. While there have been many studies on nitrogen (N_2) and methane (CH_4) plasmas, there is limited understanding on how changing operating conditions (i.e., plasma power, operating temperature) affect the plasma properties and ensuing plasma chemistry. In this work, we characterize the plasma using electrical measurements and optical emission spectroscopy (OES) and analyze the chemical products using gas chromatography to understand the effects of varying plasma parameters on plasma characteristics and product formation. Relevant electrical properties and thermodynamic information such as electron density, vibrational temperatures, as well as the presence of key plasma species (C-N, C-H, N_2) are compared to relevant products formed during plasma-alone reactions. Results show that different operating conditions lead to changes in energy partitioning in the reaction. Specifically, an increase in temperature leads to a reduction in methane conversion which appears to have an inverse relationship with the vibrational temperatures of C-H species in the plasma and could be due to changes in the permittivity of the dielectric.

I-03. Grating Optimization for Smith-Purcell Radiation: Direct Correlation between Spatial Growth Rate and Starting Current*

Md Arifuzzaman Faisal and Peng Zhang

Department of Electrical and Computer Engineering, Michigan State University, East Lansing, USA
(pz@egr.msu.edu)

Smith-Purcell radiation (SPR) is generated when electrons travel close to a metallic periodic grating (Figure 1) [1]. The operating frequency of SPR changes with different grating parameters according to the cold-tube dispersion relation [2], [3] when the grating period is fixed. We demonstrate that the spatial growth rate of SPR calculated from the hot-tube dispersion relation has the same scaling dependence on the grating parameters as the starting current calculated from PIC simulations [4], as shown in Figure 2. Thus, we confirm that the grow rate calculation using hot-tube dispersion relation can be used to predict the optimal grating parameters to minimize the starting current of SPR. This approach has a significantly reduced computation cost compared to direct PIC simulations. Both the cold-tube and hot-tube dispersion relations can be used in combination to minimize the starting current at a desired radiation frequency. While we apply our analysis to the effects of grating parameters on SPR, we expect our dispersion relation approach for grating optimization is applicable to study linear free-electron beam based vacuum devices in general, and in various geometries (e.g. cylindrical geometry).

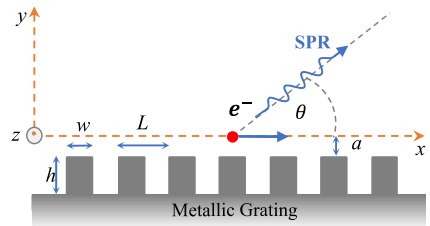

Figure 1 - Schematic of Smith-Purcell grating and electron beam configuration.

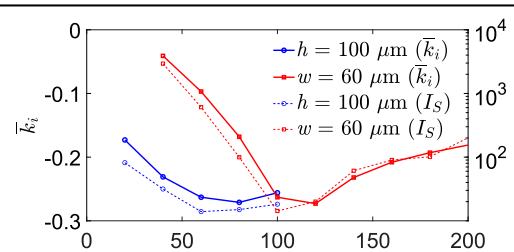

Figure 2 - Imaginary part of wavenumbers and the corresponding starting current values obtained from PIC simulations [4] as a function of the groove height *h* (squares, groove width *w* fixed at 60 μm) as well as groove width *w* (rounds, groove height *h* fixed at 100 μm).

* This work was supported in part by the Air Force Office of Scientific Research (AFOSR) YIP Grant No. FA9550-18-1-0061, the Office of Naval Research (ONR) YIP Grant No. N00014-20-1-2681, and the Air Force Office of Scientific Research (AFOSR) Grant No. FA9550-20-1-0409.

References

[1] S. J. Smith and E. M. Purcell, "Visible Light from Localized Surface Charges Moving across a Grating," *Phys. Rev.*, vol. 92, no. 4, pp. 1069–1069, Nov. 1953, doi: 10.1103/PhysRev.92.1069.
[2] P. Zhang, B. Hoff, Y. Y. Lau, D. M. French, and J. W. Luginsland, "Excitation of a slow wave structure," *Phys. Plasmas*, vol. 19, no. 12, p. 123104, Dec. 2012, doi: 10.1063/1.4771678.
[3] Y. Y. Lau and D. Chernin, "A review of the ac space-charge effect in electron–circuit interactions," *Phys. Fluids B Plasma Phys.*, vol. 4, no. 11, pp. 3473–3497, Nov. 1992, doi: 10.1063/1.860356.
[4] P. Zhang, L. K. Ang, and A. Gover, "Enhancement of coherent Smith-Purcell radiation at terahertz frequency by optimized grating, prebunched beams, and open cavity," *Phys. Rev. Spec. Top. - Accel. Beams*, vol. 18, no. 2, p. 020702, Feb. 2015, doi: 10.1103/PhysRevSTAB.18.020702.

I-04. Model for Impact of Wall Material on ECR Magnetic Nozzle Operation

Salvatore Baldinucci [a], Benjamin Wachs [b], Benjamin Jorns [b]

(a) University of Michigan, Applied Physics Department (salbal@umich.edu)
(b) University of Michigan, Aerospace Engineering department (bwachs@umich.edu, bjorns@umich.edu)

The operation of an electron cyclotron resonance magnetic nozzle thruster is modeled using a quasi one-dimensional analytical discharge model. This model builds on the helicon thruster first proposed by T. Lafleur [1], which uses semi-empirical 1D mass and momentum conservation equations coupled to a 0D energy conservation equation, to predict thruster performance. This model has been augmented by the addition of a polytropic law for the electron heat flux downstream in the expanding magnetic nozzle and the inclusion of secondary electron emission in the sheath region. Measurements are performed of both the thrust and plasma properties within the magnetic nozzle. Data from these measurements are used to inform a regression model to infer multiple parameters including the polytropic index and secondary electron emission yields for different materials.

References

[1] T. Lafleur, Phys. Plasmas 21, 043507 (2014).

I-05. Identifying Governing ODEs in Irregular Physical Domain with Diffusion*

Gina Vasey [a], Kristian Beckwith [b], Patrick Knapp [b], William Lewis [b], Brian O'Shea [a], Andrew Christlieb [a], Ravi Patel [b], Christopher Jennings [b]

(a) Michigan State University (vaseygin@msu.edu)
(b) Sandia National Laboratories

Simulating the complex plasmas created in experiments performed on the Z-Machine at Sandia National Laboratories is challenging due to both the range of spatio-temporal scales and the poorly constrained physical models needed to describe the system. In addition, the transient nature of the pulsed power drive results in a lack of a physically meaningful average or steady state about which the physical system could be linearized. Overall, this means that applying existing reduced order models (ROMs) to these transient, multi-scale, multi-physics systems presents a severe challenge. Here we develop a ROM for simulation data of 1D magnetic diffusion through a slab of finite resistivity. This problem addresses challenges regarding sharp boundaries and transient dynamics within the domain of interest. Making use of proper orthogonal decomposition (POD) coupled with the Sparse Identification of Nonlinear Dynamics (SINDy) model discovery method, we recover ordinary differential equations describing system evolution with varying amounts of problem periodicity. Finally, we examine the effects of noise and physics constraints when recovering this behavior.

* SNL is managed and operated by NTESS under DOE NNSA contract DE-NA0003525. SAND2022-9174 A

I-06. Development of a Microstrip Half-Wave Split-Ring Resonator for Microwave-Assisted Laser-Induced Breakdown Spectroscopy and Laser Ablation Molecular Isotopic Spectrometry*

Kelsey L. Williams and Steven J. Ray

The State University of New York at Buffalo (kelseywi@buffalo.edu, sjray2@buffalo.edu)

Laser-induced breakdown spectroscopy (LIBS) is a well-established measurement technique in which a laser is focused onto the surface of a sample resulting in formation of a laser-induced plasma (LIP). Atomic emission spectrometry then allows for quantitative analysis of the sample. Emission from a LIP is temporally-dependent. Early in the plasma lifetime emission is dominated by continuum background, however, as the LIP dissipates, continuum background decreases and atomic emission dominates the spectrum. As the LIP cools further, molecular diatomics form as a consequence of the interaction of plasma species and the surrounding atmosphere. A relatively new technique known as laser ablation molecular isotopic spectrometry (LAMIS) measures emission from these excited diatomic species in order to evaluate the isotopic composition of the sample based upon the different wavelengths of the vibronic band-head of each isotopologue.

Recently, several methods have been reported that use microwave energy to improve the limits of detection of typical LIBS experiments by using microwaves to extend the lifetime of the plasma. A variety of experiments using the Beenakker waveguide cavity, simple loop antennas, or near-field applicators have reported up to 1000-times improvement in signal for atomic emission.[1-3] Although these techniques have been successful, little is known as to the influence of the microwave field on the LIP, nor the role of the microwave field intensity, structure, or duration on the plasma/microwave field coupling.

In this work, we develop and investigate the efficacy of a microstrip half-wave split-ring resonator as an experimental method to improve microwave application to the LIP.[4] Microstrips are cheap and simple to fabricate through a chemical etching process, and the dimensions of the resonator can be tuned to match the overall impedance of the system. The resonator used here is a ring with a gap on one side where the LIP is formed, with the dimension calculated to resonate at ½ the wavelength of the microwave frequency in use (2.45 GHz). The efficacy of this approach to enhance LIBs and LAMIS experiments will be evaluated.

* NSF Grant PHY-2206546 (RAY)

References:

[1] Y. Liu, B. Bousquet, M. Baudelet, and M. Richardson, Spectrochimica Acta Part B **73**, 89 (2012).
[2] M. Tampo, M. Miyabe, K. Akaoka, M. Oba, H. Ohba, Y. Maruyama, and I. Wakaida, Journal of Analytical Atomic Spectrometry **29**, 886 (2014).
[3] M. Wall, Z. Sun, and A. T. Alwahabi, Optics Express **24**, 1507 (2016).
[4] F. Iza and J. A. Hopwood, IEEE Transactions on Plasma Science **31**, 782 (2003).

I-07. Correlations between Empirical and Self-consistent Anomalous Transport Models in Hall Thrusters

Thomas A. Marks and Benjamin A. Jorns

University of Michigan, Ann Arbor, MI, 48109 (marksta@umich.edu)

The development of fully predictive simulations of crossed-field plasma discharges such as Hall effect thrusters is a longstanding goal of the low temperature plasma propulsion community. This goal is hindered by the presence of unknown physics in these devices, such as the presence of enhanced "anomalous" cross-field electron transport. One common way to address this in practice is to tune a constant anomalous transport profile along the thruster centerline such that the simulation output matches experimental data[1].

For a long time, empirical profiles produced in this way have been treated as surrogate measurements of the actual anomalous transport in the Hall thruster discharge. In a previous work, we used a dataset of such profiles in combination with a symbolic regression algorithm to try and discover new models of the anomalous transport However, despite the fact that such models fit empirical profiles quite well, even for thrusters and operating conditions not in their training dataset[3], they performed poorly when implemented self-consistently into a Hall thruster simulation. This suggests that empirical profiles may not actually correlate well with the true anomalous transport profile in Hall thrusters and that they may represent only a single, non-unique solution.

In this work, we attempt to determine whether this is true. We look at three test cases, A, B, and C, in which we train a first-principles[3], data-driven[2], and reverse empirical model, respectively to a reference simulation of the H9 Hall thruster. We find that how well a model fits an empirical profile has little relevance for how well the model performs when integrated into a simulation, suggesting that the use of such profiles in theoretical work may not be justifiable.

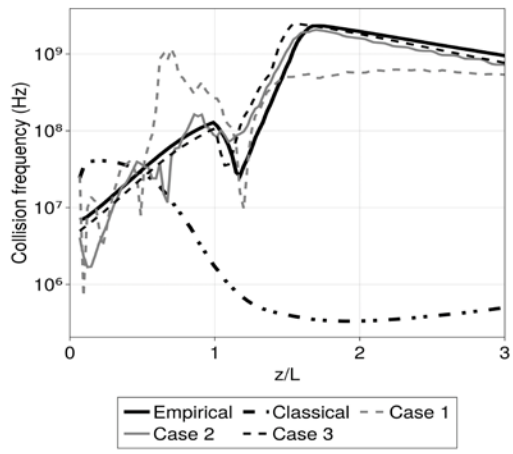

Figure 1 – Comparison of anomalous transport models to empirical reference data

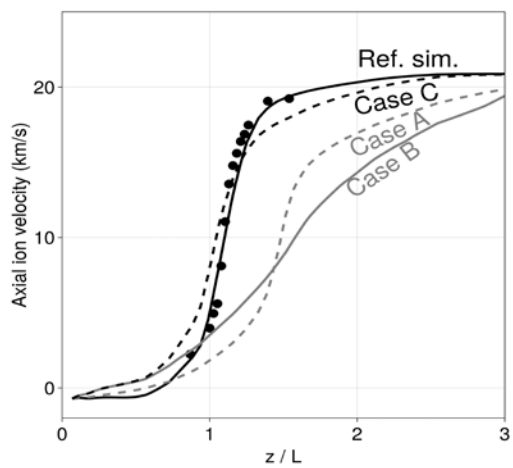

Figure 2 – Ion velocity profiles resulting from models in Fig. 1 being implemented self-consistently into Hall thruster simulation

References

[1] I. Mikellides and A. Lopez Ortega. PSST **28**, 1 (2019).
[2] B. Jorns, Plasma Sources Sci. Technol. 27 104007 (2018)
[3] T. Lafleur et al. Physics of Plasmas 23, 053503 (2016)

I-08. Resolving Extended Space and Time Correlations in Molecular Dynamics Simulations of Strongly Magnetized Plasmas*

Julia L. Marshall, Louis Jose and Scott D. Baalrud

University of Michigan Department of Nuclear Engineering and Radiological Sciences (julm@umich.edu)

Strongly magnetized plasmas are characterized by having a gyrofrequency larger than the plasma frequency. In this regime, the motion of charged particles is constrained to small cylinders with a width characterized by the gyroradius and a length characterized by the collision mean free path. Recent molecular dynamics simulations showed that this channeling effect leads to increased temporal and spatial correlations associated with Coulomb collisions. [1] These simulations used cubic domains, which significantly limited the range of magnetization strength that they could explore because it required a large number of particles to resolve the long-range correlations. Here, we show that an elongated domain in the direction of the magnetic field can capture the effects with significantly fewer particles than a cubic domain. We define a unit cubic domain by the size needed to capture weakly magnetized plasmas, then elongate the domain by adding additional cubes in the direction parallel to the magnetic field. A proof of principle is demonstrated by computing the self-diffusion tensor of the strongly magnetized one-component plasma using the velocity autocorrelation function.

*This research was supported by US Department of Energy grant no. DE-SC0022202, and in part through computational resources and services provided by Advanced Research Computing (ARC), a division of Information and Technology Services (ITS) at the University of Michigan, Ann Arbor.

References

[1] K. Vidal, S. Baalrud, Phys. Plasmas 28, 042103 (2021).

I-09. Non-thermal Plasma Synthesis of Hydrophobic Silicon Nanoparticles

Sankhadeep Basu [a], Gabriel Ceriotti [b] Cameron Papson [c] and Rebecca Anthony [c]

(a) Chemical Engineering and Material Science Department, Michigan State University (basusank@msu.edu)
(b) Electrical and Computer Engineering Department (ceriott2@msu.edu)
(c) Mechanical Engineering Department, Michigan State University (ranthony@msu.edu)

Hydrophobic nanomaterials have drawn significant attention due to their applications in coatings, protein adsorption, nanomedicines, etc[1]. For silicon nanomaterials, researchers have generally used external agents which react with the surface terminated Si-H bonds and render the surface hydrophobic. In the present work we investigate the hydrophobic nature of as-prepared silicon nanoparticles (SiNPs) produced in a nonthermal plasma reactor. SiNPs were synthesized in a flow-through reactor using silane with argon as the background gas. The total gas flowrate was 20 standard cubic centimeters per minute (sccm) and with a reactor pressure of 1.4 Torr. The plasma as generated using radiofrequency (rf) power of 10W at 13.56 MHz is delivered via ring electrodes encircling the reactor. SiNPs formed in the plasma were collected on a stainless-steel mesh filter at the reactor exhaust. Further examination under Scanning Electron Microscopy (SEM) revealed the formation of flow-through aggregated wires of around 12 microns in length and 7-8 microns in diameter, comprised of primary SiNPs. Transmission electron microscopy showed the primary particle size to be in range of 5-7 nm, but no electron diffraction rings were detected, indicating that the Si NPs were amorphous. Contact angle measurements were performed to test the hydrophobicity of the as-prepared SiNPs. A water contact angle of 146˚ was observed demonstrating the near-superhydrophobic (> 150˚) nature of the aggregated SiNPs. The hydrophobic material was also successful in separating both vegetable cooking oil as well as heavy-duty pump oil from oil-water mixtures. Thermal experiments were also performed to illustrate the thermal stability of the hydrophobic nature. The nanomaterial was able to retain its hydrophobicity even at 450˚C after 2h of heating showing robust stability. The material was also found to be stable under ambient air conditions as water contact angle did not change significantly even after a week of synthesis. These exciting properties signify the future prospects in coatings, biotechnology and more.This work was supported by NSF CMMI Career 1651674.

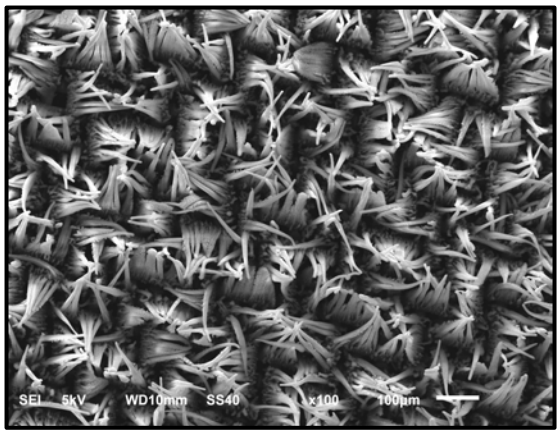

Figure 1 – Scanning Electron Microscopy image of synthesized silicon nanostructures

References

[1] Hoshian et al., ACS Appl. Mater. Interfaces, **7**, 1 (2015).

I-10. A Hydrodynamic Mechanism for Hot Spot Formation in the Remnant of SN1987A*

Michael Wadas [a], Heath LeFevre [b], Aaron Towne [a], Carolyn Kuranz [b], and Eric Johnsen [a]

(a) Mechanical Engineering, University of Michigan, Ann Arbor, MI (mwadas@umich.edu)
(b) Nuclear Engineering & Radiological Sciences, University of Michigan, Ann Arbor, MI

Since the light from supernova 1987A (SN1987A) first reached Earth, the evolution of the dying star has been the subject of intense study [1]. In particular, several theories have been proposed to explain the formation of hot spots, or accumulations of mass, along the ring of gas surrounding the supernova origin [2, 3]. In this study, we assess the viability of a hydrodynamic mechanism related to the stability of interacting vortex cores (Crow instability) in explaining the formation of the mass accumulations [4]. Perturbations along the circular cores, which would have formed when the progenitor star emitted the ring of gas approximately twenty-thousand years prior to the supernova, grow under the influence of their self- and mutually induced velocity fields. Once the perturbations reach a magnitude on the order of the core separation distance, the cores touch, triggering a complex vortex reconnection process that ultimately results in a series of smaller vortex rings.

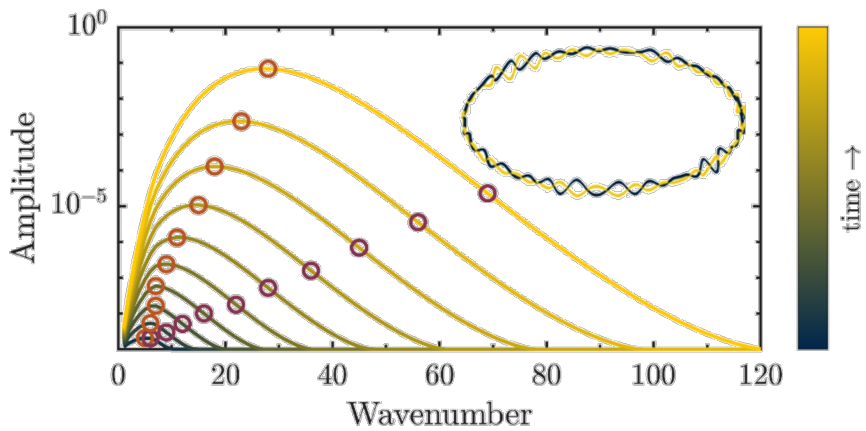

Figure 1 - Perturbation spectra at various times showing the mode with the greatest amplitude (orange symbols) and the mode with the greatest growth rate (purple symbols). Inset shows an inverse Fourier transform of the spectra at the last time.

Unlike the classical stability analysis, which concerns infinite planar line vortices [4], the zero-order motion of the flow causes the growth rates of different modes to vary in time. An accurate prediction of the mode that emerges in practice must therefore consider the time-integrated growth of the modes. The figure shows spectra at several times showing the mode of greatest amplitude along with the mode with the greatest growth rate. The inset shows an inverse Fourier transform of the spectrum at the latest time when the mode selection is made. Our analysis predicts a dominant instability wavenumber consistent with the number of observed hot spots surrounding SN1987A, thus providing evidence in support of the present formation mechanism. The present results have important implications for nebula formation following supernovae as well as the role of vorticity dynamics in astrophysical flows.

* This work is funded by the U.S. Department of Energy (DOE) NNSA Center of Excellence under cooperative agreement number DE-NA0003869 and by the U.S. DOE NNSA Stewardship Science Graduate Fellowship under grant DE-NA0003960.

References

[1] Dotani et al., Nature Lett. 330 (1987) 230. [2] Fransson et al., Astrophys. J. Lett. 806 (2015) L19.
[3] Kang et al., Phys. Rev. E. 64 (2001) 047402. [4] Crow, AIAA J. 8 (1970) 12.

I-11. Relativistic Laser Perturbation to Laser-Driven Magnetic Reconnection*

Joshua Latham,[a] Brandon K. Russell,[a] Paul T. Campbell,[a] Louise Willingale,[a] Gennady Fiksel,[a] Philip M. Nilson,[b] Karl M. Krushelnick [a]

(a) Center for Ultrafast Optical Science (CUOS), University of Michigan (joshla@umich.edu)
(b) Laboratory for Laser Energetics, University of Rochester

Experiments which measure the magnetic fields laser-driven plasmas give insight into the basic processes of plasmas such as magnetic reconnection [1]. These processes become more difficult to describe when there is a mixture between regimes [2], such as between relativistic kinetic plasma and MHD-describable plasma, as in this case.

In this experiment, a 10-ps, 10^19 W/cm^2 infrared (IR) laser impinged on the interface between two plasma plumes driven by 2.5 ns, 10^14 W/cm^2 ultraviolet (UV) lasers at the OMEGA-EP laser facility. The magnetic fields were measured with proton radiography from a TNSA source. In one regime, the relativistic perturbation inhibited the magnetic reconnection between the two plasma plumes, but with a different timing of the relativistic laser the reconnection may have been enhanced. Probable causes will be discussed. This work is relevant to understanding the physics of reconnection in HED plasmas.

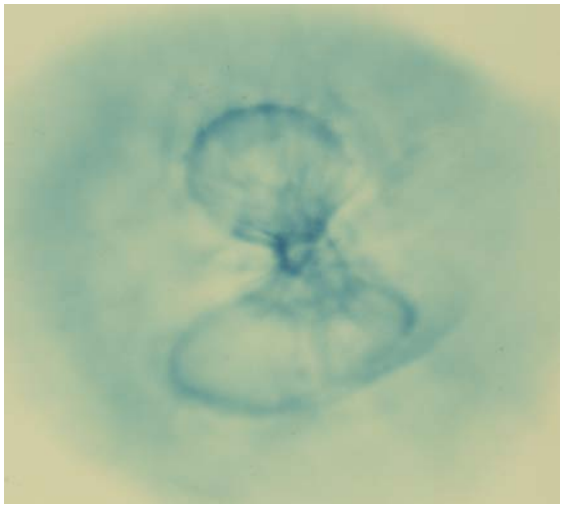

Figure 1 – 16.5 MeV proton image of the variations in magnetic field. In this case, the IR laser hit the target 0.3 ns after the start of the UV pulses, and the image was taken 0.6 ns after the IR strike.

* The experiment was conducted at the Omega Laser Facility with the beam time through the National Laser Users' Facility (NLUF) (or the Laboratory Basic Science) under the auspices of the U.S. DOE/NNSA by the University of Rochester's Laboratory for Laser Energetics under Contract DE-NA0003856

References

[1] P. M. Nilson *et al.*, Phys. Rev. Lett., **97**(25), 255001, (2006).
[2] H. Ji *et al.*, Nat. Rev. Phys., **4**, 263-282 (2022).

I-12. Nonthermal Plasma Synthesis of Carbon Nanodots

Cameron Papson, Sankhadeep Basu, Tanvi Nikhar, Sergey Baryshev, Rebecca Anthony

Michigan State University Engineering Department (papsonca@msu.edu)

In recent years, Carbon nanodots (CDs) have been of great interest for their applicability in areas such as solar energy harvesting, nano-sensing, photocatalysis, etc. Traditional routes for synthesis for CDs involve both top down methods like laser ablation, electrochemical synthesis, and chemical oxidation, as well as bottom up techniques like hydrothermal synthesis, microwave pyrolysis and others. In this work we report the synthesis of CDs in a nonthermal radiofrequency plasma reactor using methane as the carbon precursor. Nonthermal plasma synthesis offers several advantages over traditional routes in terms of simplicity, solvent free synthesis and near room temperature growth of nanoparticles. Radiofrequency power at 13.56 MHz was supplied through ring electrodes to a flow-through reactor tube held at 2.9 Torr. The CDs formed in the plasma were deposited onto arbitrary substrates via inertial impaction. The synthesized material was characterized using Transmission Electron Microscopy (TEM), Scanning Electron Microscopy (SEM), Raman spectroscopy, and UV-Vis optical absorption. Raman spectroscopy exhibited two significant features; the D band around 1330 cm^{-1} and the G band around 1590 cm^{-1}. While Raman spectroscopy did not reveal significant modifications in the bonding configuration upon changing synthesis parameters, by controlling the hydrogen content in the plasma via introduction of H_2 gas, there arose a dramatic shift in the visual appearance, nanostructure, and UV-Vis optical absorption. Under hydrogen-poor conditions, the CDs were black and accompanied by optical absorption across the visible range, while hydrogen-rich conditions led to white-appearing CD powders with an onset of optical absorption in the UV. TEM image analysis indicated that the average particle size was around 6nm under hydrogen-poor conditions, and much larger at >40nm for hydrogen-rich conditions. Additionally, the black CDs appeared to be in nano-onion-like morphologies, as evidenced with TEM imaging, while the white CDs appeared entirely amorphous with no layered structure within the primary particles, consistent with highly diversified sp-2 and sp-3 bonding within the CDs. Our future work will quantify the degree of sp-3 hybridization for CDs of both varieties, as well as measuring the effect of hydrogen during synthesis on the electrical conductivity of CD films created by inertial impaction directly from the reactor.

I-13. Frequency-Selective Plasma Limiters

Sandeep Narasapura Ramesh and Abbas Semnani

The University of Toledo, Toledo, Ohio
(sandeep.narasapuraramesh@rockets.utoledo.edu , abbas.semnani@utoledo.edu)

Frequency selective limiters traditionally operate by rejecting/reflecting unwanted high-power frequency signals. This results in both the stop-band rejection level (isolation) and bandwidth of the limiter being dependent on the resonator's quality factor. On the other hand, an absorptive limiter that absorbs unwanted high-power frequencies can provide a very high level of stopband rejection and bandwidth.

This paper introduces a novel frequency selective absorptive limiter utilizing a plasma shell. An absorptive topology includes two resonators, a phase delay line, and plasma for inter-resonator coupling. They operate by creating two signal paths and introducing a phase difference to either produce constructive or destructive interference depending on the desired response. When the input power is high, there is a plasma breakdown, finite inter-resonator coupling, and the phase difference between the signals is 180 deg resulting in destructive interference. This results in a limiter with theoretically infinite stop-band rejection. However, when the input power is low, there is no breakdown, no inter-resonator coupling, and the phase difference results in constructive interference resulting in an all-pass behavior.

We implemented the topology on PCB using two quarter-wave resonators and commercially available Gas Discharge Tubes (GDTs) as the plasma shells. The fabricated device performed in agreement with the theory and simulations with over 60 dB isolation during the band stop state and 1.5 dB insertion loss during the all-pass state.

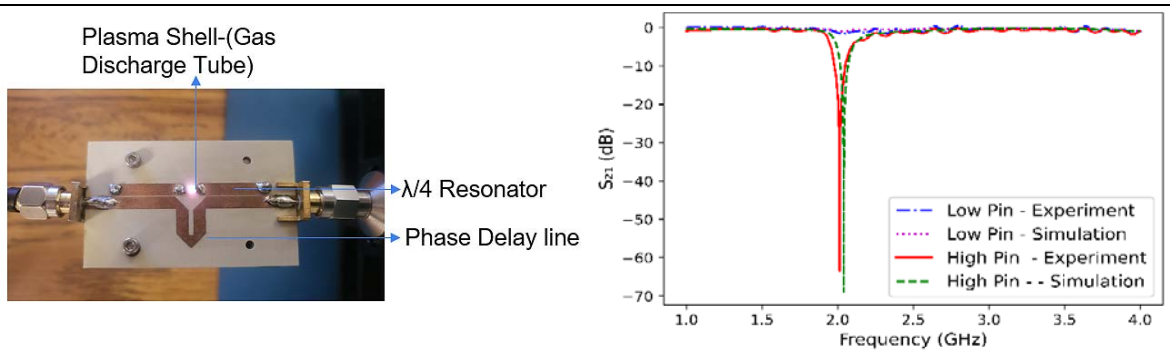

Figure 1 – A prototype of frequency-selective plasma limiter and its measure transmission coefficient in plasma OFF and ON modes.

* Work supported by ONR Grant No. N00014-21-1-2441.

References

[1] M. Hickle and D. Peroulis, J. IEEE Transactions on Circuits and Systems. VOL **65**, No **6** (2018).
[2] A. Semnani, S.O. Macheret, and D. Peroulis, IEEE Transactions on Plasma Sciences. VOL **44**, No **12** (2016)
[3] S.N. Ramesh and A. Semnani, IEEE Transactions on Plasma Sciences. VOL **49**, No **14** (2021).

I-14. Femtosecond Laser Formation of NV centers in Diamond and STED Microscopy Characterization*

Farha Islam Mime [a], Gabriel Ceriotti [a], Timothy A. Grotjohn [a] and Marcos Dantus [b]

(a) Department of Electrical and Computer Engineering, Michigan State University, East Lansing, Michigan 48824, USA (mimefarh@msu.edu)
(b) Department of Chemistry, Michigan State University, East Lansing, Michigan 48824, USA

Nitrogen-Vacancy (NV) centers in diamond consist of a substitutional nitrogen atom and an adjacent vacancy and they are a promising solid-state system for implementing quantum bits (qubits) and as quantum sensors. This is because of their exceptional electron spin characteristics at room temperature as well as their capability as single photon emitters. The creation of NV centers at predetermined locations presents a key challenge to quantum systems application. An effective method to create vacancies at specific positions with greater accuracy is provided by laser writing which utilizes a highly focused femtosecond laser spot to displace carbon atoms from the lattice in diamond [1]. The number of vacancies generated by this method can be effectively controlled by adjusting the laser parameters [2]. This work demonstrates the creation of NV centers in nitrogen-doped diamond at deterministic positions through femtosecond laser irradiation. To resolve NV centers in diamond with sub-50 nm spatial resolution, Stimulated Emission Depletion (STED) microscopy [3], a super-resolution microscopy technique that breaks the diffraction limit of light is being built. The implementation and performance of the STED microscopy applied to NV centers will be presented.

* This work is supported by Strategic Partnership Grant (SPG) by the Michigan State University Foundation.

References

[1] T. Kurita, N. Mineyuki, *et al*., Appl. Phys. Lett. 113, 211102 (2018).
[2] Y.-C. Chen, *et.al*, Nature Photonics, 11 (2017) 77-80.
[3] S. W. Hell and J. Wichmann, Opt. Lett. 19, 780-782 (1994).

I-15. Hybrid Optimization Method for Parameter Fitting in High Aspect Ratio Etching*

Florian Krüger [a], Minjoon Park [b], Andrew Metz [b] and Mark J. Kushner [a]

(a) University of Michigan, 1301 Beal Avenue, Ann Arbor, MI 48109-2122, USA (fkrueger@umich.edu, mjkush@umich.edu)
(b) TEL Technology Center, America, LLC, 255 Fuller Road, Suite 214, Albany, NY 12203 USA

Computational investigations of plasma etching of structured micro and nano electronics are highly dependent on precise knowledge of a variety of coefficients to accurately represent the physical behavior of these processes. The increased complexity of the final structures and introduction of novel gas compositions coupled with the necessarily reduced reaction set used by numerical investigation makes it extremely difficult to choose these critical parameters. This problem is further exacerbated by the fact that many of the involved physical and chemical processes are based on entirely different fundamental principles i.e., sputtering, chemical etching, chemisorption, physisorption etc.

The aim of this work was to automate the implementation of a subset of reaction rates and angular dependencies by matching them to a real process using gradient descent methods. To that end a series of etches of narrow SiO_2 features using a C_4F_6 / C_4F_8 / CH_2F_2 /O_2 plasma is performed and relevant quantities such as etch depth, etch rate, aspect ratio as well as critical widths at several depths are determined using scanning electron microscopy.

Thereafter, the same process was reproduced using Monte Carlo Feature Profile Model (MCFPM). Some of the input parameters used by MCFPM were coupled to a multi variate gradient descent cycle that iteratively optimized relevant input parameters in order to achieve the best match between simulation and experiments.

We were able to demonstrate that using these methods a good agreement between the real-world result and the simulation output can be achieved.

* Work supported by Tokyo Electron and the National Science Foundation.

I-16. Exploring the Importance of Temperature-Dependent Opacities in the Modeling of X-Ray Induced Thermomechanical Shock Experiments*

Julian Kinney [a], Peter Porazik [b], Steve Moon [b], Israel Lopez [b], Carolyn Kuranz [a]

(a) University of Michigan (julkin@umich.edu)
(b) Lawrence Livermore National Laboratory

Absorption of high intensity X-rays in solid materials produces a thermomechanical response. Recently, experiments on the National Ignition Facility (NIF) were performed to study the response for a variety of materials and source spectra. Computational modeling of these experiments is difficult due to the wide array of physical phenomena involved over a range of differing timescales.

This study first validates the simulation results with experimental data for both unfiltered and filtered samples and then compares the results with well-known theoretical models. X-ray absorption increases the temperature of materials, changing the opacity, and thus feeding back to affect the energy deposition. We explore and quantify the effect of the temperature-dependent opacities on the overall material response. In the end, this work aims to answer whether changes in opacity during the energy deposition process are important for accurate modeling of the material response.

* This work was supported in part by the Lawrence Livermore National Laboratory under subcontract B642551.

II-01. A Discrete Cavity Analysis of Coupled-cavity Travelling Wave Tubes*

Ayush Paudel [a], Peng Zhang [a], Patrick Wong [a], John Luginsland [b] and Matthew Franzi [c]

(a) Michigan State University, East Lansing, Michigan, USA (pz@egr.msu.edu)
(b) Confluent Sciences, LLC. Present address: Air Force Office of Scientific Research, Arlington, Virginia, USA
(c) Air Force Research Laboratory, Albuquerque, New Mexico, USA

Coupled-cavity travelling wave tubes (CC-TWTs) are important to applications which require broad-band amplification and high gain. Classical Pierce theory [1] has treated the beam-circuit interaction as being continuous and uniform in the axial direction, which is taken to extend to infinity. However, it is important to test the limit of this treatment of beam-circuit interaction in real systems where the tubes are finite in length and discrete cavity effects may become important. Discrete cavity analysis allows us to treat individually tunable cavities, which leaves room for treating non-uniformity in the cavities that might be caused by random errors in manufacturing. The non-uniformity of cavities can be reflected in variations in resonant frequencies and shunt-impedances of the cavities.

We extend the previous preliminary work on the discrete cavity model by Wong et al [2]. An eigen-analysis method is used to obtain the cold-tube dispersion relationship for multi cavity systems, where the effects of cavity number, quality factor and cavity coupling are examined. The model is then extrapolated to include the electron beam, and the hot-tube results is currently being examined (Fig. 1). The relationship between this type of analysis and the classical Pierce analysis will also be discussed by attempting to recreate the results from [3].

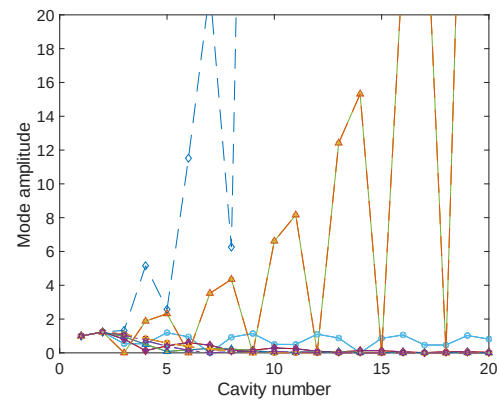

Figure 1 – Progression of cavity voltage as the beam passes through a 20 cavity CC-TWT.. Cavity resonant frequency $\omega_0 = 2\pi \times 8\ GHz$, operation frequency $\omega = 2\pi \times 7\ GHz$, cavity coupling constant, $c = 0.19$, beam current $I = 40\ A$, beam energy = $100\ keV$. Different curves represent the results for different wavenumbers determined from the hot-tube dispersion relation.

*Work supported by Air Force Office of Scientific Research (AFOSR) YIP Grant No. FA9550-18-1-0061, The Office of Naval Research (ONR) YIP Grant No. N00014-20-1-2681, and Air Force Office of Scientific Research (AFOSR) Grant No. FA9550-20-1-0409. JWL's work was performed in part while working with Confluent Sciences, LLC under contract to AFRL/RD.

References

[1] J. R. Pierce, Traveling Wave Tubes, Van Nostrand: New York, NY, USA (1950)
[2] P. Wong, P. Zhang, and J. Luginsland, "Recent theory of traveling-wave tubes: A tutorial-review," *Plasma Res. Exp.*, vol. 2, no. 2, 2020, Art. no. 023001, doi:10.1088/2516-1067/ab9730
[3] Hoff B. W., Simon D. S., French D. M., Lau Y. Y. and Wong P., 2016," Study of a high power sine waveguide traveling wave tube amplifier centered at 8 GHz", *Phys. Plasmas*, 23, 103102.

II-02. Data-driven Modelling of Laser-plasma Experiments Enabled by Large Datasets

Andre F Antoine, Archis Joglekar and Alexander GR Thomas

University of Michigan, Ann Arbor, MI (aantoine@umich.edu, archisj@umich.edu, agrt@umich.edu)

Laser Wakefield Acceleration (LWFA) is a process by which high gradient plasma waves are excited by a laser leading to the acceleration of electrons. The process is highly nonlinear leading to difficulties in developing 3 dimensional models for a priori, and/or ab initio prediction.

Recent experiments at the Rutherford Appleton Laboratory's (RAL) Central Laser Facility (CLF) in the United Kingdom using the 5Hz repetition rate Astra-Gemini laser have produced new results in LWFA research, inviting analysis of data with unprecedented resolution. Additionally, data driven modeling, scaling laws and models can be extended into new ranges or refined with less bias.

We will present results of training deep neural networks to learn latent representations of experimental diagnostic data and valídate the latent space by comparing the distribution of beam divergences and other metrics of randomly generated spectra against the distribution in the training data. We will discuss the ability of the model to generalize results to different conditions. This work will use architectures which rely on reparameterization using a small dense network connected to a larger, convolutional neural network.

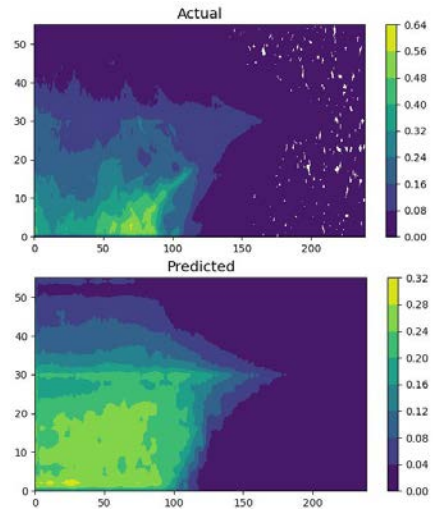

Figure 1 – Example of electron angle – energy spectra. The above is a true experimental measurement, and below is a prediction of the same spectrum.

* Work supported by the NSF.

II-03. Non-thermal Plasma Jet Sintering of Indium Tin Oxide Thin Films

Zhongyu Cheng [a], Ali Newaz Mohammad Tanvir [a], Jinyu Yang [a], Yanliang Zhang [a] and David B. Go [a, b]

(a) Department of Aerospace and Mechanical Engineering (zcheng5@nd.edu)

(b) Department of Chemical and Biomolecular Engineering (dgo@nd.edu)

University of Notre Dame, Notre Dame, IN, 46556 USA

Indium tin oxide (ITO) is a widely used thin-film material, due to its electrical conductivity and optical transparency. It is a good candidate material for flexible electronics, solar cell panels, and touch screens. Therefore, it is important to develop an effective method to process ITO thin films. Non-thermal plasma jet sintering is a technique for sintering printed nanoparticle inks, which has previously been proven to enhance the electrical conductivity of printed silver nanoparticle thin films. It can be easily set up based on a dielectric barrier discharge (DBD) plasma jet configuration and operated under atmospheric pressure and temperature without damaging the thin films or thermally-sensitive substrates. In this research, we used blade coating to deposit ITO thin films on glass and quartz surfaces and sintered the deposited inks using an argon plasma jet. There are several key input parameters that can influence the sintering result such as sintering time, argon gas flow rate, applied voltage, gap distance between the ITO thin film surface and plasma jet, and input frequency. We are investigating the optimal input sintering conditions based on these parameters. Our current experimental result shows that the electrical conductivity of ITO thin films increased significantly after 15 minutes of plasma jet exposure. As a contrast, to achieve a similar conductivity increase, conventional sintering using a furnace required several hours, which requires longer processing time and a temperature of 800 °C.

II-04. Interaction of Atmospheric Pressure Plasma Jets with Complex Surfaces of Different Dielectrics*

Kseniia Konina [a], Sai Raskar [b], Igor Adamovich [c] and Mark Kushner [d]

(a) University of Michigan, Ann Arbor, MI 48109-2122 USA (kseniiak@umich.edu)
(b) Ohio State University, Columbus, OH 43210-1142 USA (raskar.1@buckeyemail.osu.edu)
(c) Ohio State University, Columbus, OH 43210-1142 USA (adamovich.1@osu.edu)
(d) University of Michigan, Ann Arbor, MI 48109-2122 USA (mjkush@umich.edu)

All real surfaces are usually a combination of non-planar and/or non-uniform interfaces. With the growth of interest in interdisciplinary subjects, an interaction of low-temperature plasmas with different materials gained interest in a scientific society. Understanding how simple types of complex surfaces can interact with plasmas is crucial because such interfaces are usually similar to actual patterns on surfaces.

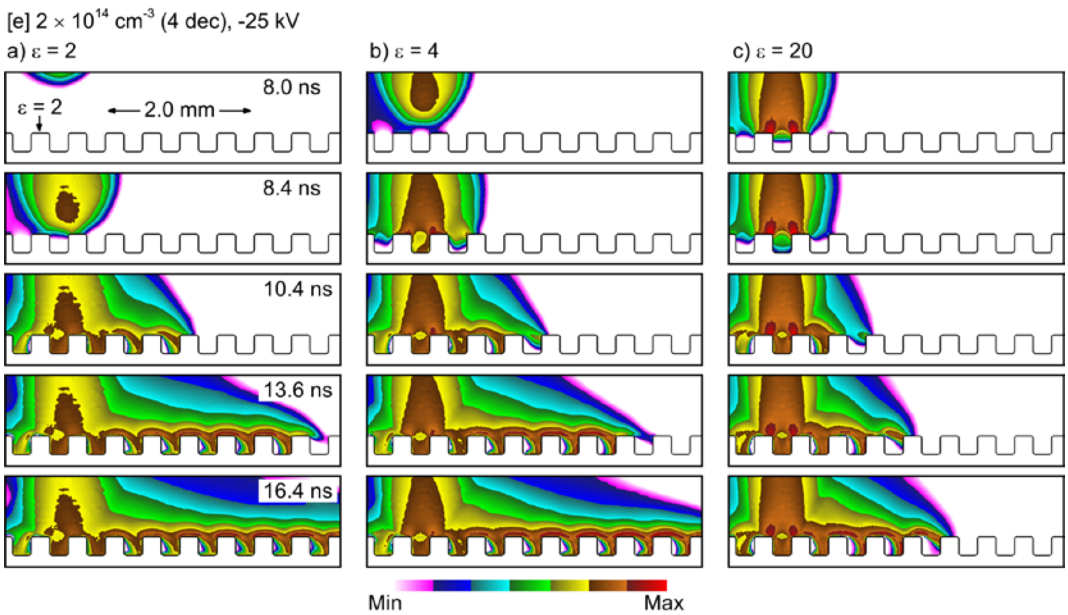

Figure 1 – Electron density evolution during plasma propagation across dielectric surface with rectangular microchannels having different dielectric permittivities.

For example, rectangular microchannels can represent the topical area of human skin. It is widely known that low-temperature plasmas have potentially different benefits in interacting with biological tissue.

In this work interaction of atmospheric pressure plasma jet with dielectric microchannels is investigated using a modelling platform *nonPDPSIM* [1] and an experimental technique to determine electric field *EFISH* [2]. Different parameters of discharge, along with various surfaces with different properties, are investigated in this work (Fig. 1).

* Work supported by the DoE Office of Fusion Energy Sciences and the NSF.

References

[1] S. A Norberg *et al*, Plasma Sources Sci. Technol. **24**, 035026 (2015).
[2] K. Orr et al, Plasma Sources Sci. Technol. **29**, 035019 (2020).

II-05. Enabling Bright Carbon Nanotube Fiber Field Emission Cathode

Taha Y. Posos [a], Jack Cook [b] and Sergey V. Baryshev [a]

(a) Michigan State University, Michigan, USA (pososta h@msu.edu)
(b) University of Cambridge, Cambridge, UK

In this work, we introduce a new technique which improves emittance of the carbon nanotube fiber field emission cathode (CNT fiber FEC) many-fold. CNT fibers remain of high interest for next generation electron source research and development as they have low turn-on voltage, high conductivity, durability, and flexibility. However, control over its emission properties is a challenge. Our previous studies showed that formation of stray emitters due to thermal and field stress during emission causes spatially non-coherent beam, which means large emittance and low brightness. It was also shown that the emission over the surface was confined to small number of stray spots, which makes most of the surface useless and leads to local hot spots, arcs, and failure of the cathode.

To prevent formation of stray emitters, we electroplated fiber ropes, made of multiple twisted CNT fibers, with nickel, then cut its top with a femtosecond laser to minimize surface ablation, and welded it on a metal base. The final structure has 150 μm fiber core, 50 μm thick Ni shell, and is 4.8 mm in height. Our emission test results showed that emission from the cathode forms a single spot comparable to the entire size of the cathode fiber core and high output current. This is an indication of high brightness and emission uniformity over the surface. Detailed results and brightness estimations will be presented.

II-06. Design and Demonstration of a Dual Frequency, Harmonic, Magnetically Insulated Line Oscillator

Ryan A. Revolinsky, Emma N. Guerin, Stephen V. Langellotti, Christopher J. Swenson, Levi I. Welch, Drew A. Packard*, Nicholas M. Jordan, Y.Y. Lau, and Ronald M. Gilgenbach

Plasma, Pulsed Power, and Microwave Laboratory (PPPML), Nuclear Engineering and Radiological Science Department, University of Michigan, Ann Arbor, MI, USA (revolins@umich.edu)
* Currently employed by General Atomics, San Diego, CA

The harmonic magnetically insulated line oscillator (HMILO) is a crossed-field, high power microwave (HPM) device that does not require an external magnet. Magnetic insulation is realized through the azimuthal magnetic field generated by axial current flow along the cathode [1]. The HMILO attains dual frequency operation utilizing a single source, single cathode, and dual slow wave structure (SWS) at L-band (~1 GHz) and S-band (~2 GHz), as shown in Figure 1.

Design of the HMILO combined the explicit Brillouin flow solutions, unit-cell cold tube simulations, and Particle-in-Cell (PIC) simulations [1] [2] [3].

Figure 2 shows experimental results of HMILO operation, with driver parameters of 256 kV and 9.9 kA generating 12.7 ± 7.6 MW microwave power with a dominant frequency of 0.984 ± 0.013 GHz for LBO filtered extraction. For SBO extraction operational driver parameters were measured to be 238 kV and 8.6 kA generating 3.2 ± 1.5 MW microwave power with a dominant frequency of 2.074 ± 0.003 GHz.

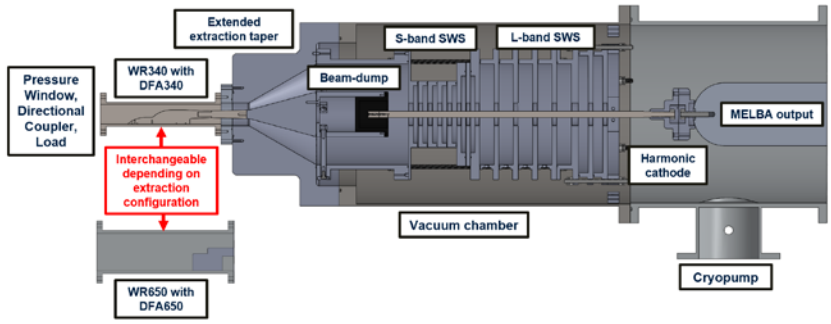

Figure 1 – CAD model of HMILO experimental configuration.

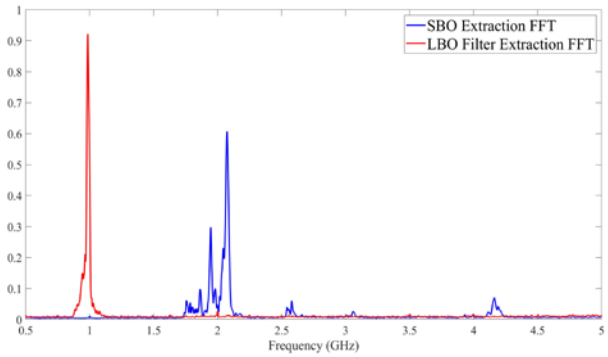

Figure 2 – Frequency spectrum of two nominally-identical HMILO pulses using different extraction hardware.

* This work was supported by the Office of Naval Research (ONR) Award #N00014-19-1-2262, and by L3Harris Electron Device Division.

References

[1] D. A. Packard, et al., *Phys. Plasmas*, vol. 28, p. 123102, Dec. 2021.
[2] Y. Y. Lau, et al., *IEEE Trans. Plasma Sci.*, vol. 49, p. 3418, Nov. 2021.
[3] D. A. Packard, et al., *IEEE Trans. Plasma Sci.*, vol. 48, p. 1894, Jun. 2020

II-07. Microwave Plasma Assisted Chemical Vapor Deposition Process Variable Optimization of Nitrogen Doped Single Crystal Diamond

Sarah P. Roberts [a], Alex Loomis [a], Nathan Jansen [a], Aaron Hardy [b], Jonas N. Becker [a,b], Shannon S. Nicley [a,b]

(a) Quantum Optical Devices (QuOD) Lab, Michigan State University, 567 Wilson Rd, East Lansing, MI 48824 (rober964@msu.edu)

(b) Fraunhofer USA Inc. Center Midwest (CMW) Division for Coatings and Diamond Technologies, 1449 Engineering Research Ct., East Lansing, MI 48824, USA

The nitrogen vacancy defect (NV^-) in diamond is a strong quantum information bit (qubit) candidate for quantum sensing applications. Though many researchers have demonstrated success in utilizing the NV^- defect for sensing temperature [1] and magnetic field [2], the challenge of repeatably manufacturing NV^- defects has not been thoroughly addressed. Here, a parametric study of a microwave plasma assisted chemical vapor deposition (MPACVD) reactor was performed to understand the effects of substrate temperature and reactor pressure on the incorporation of nitrogen in single crystal diamond (SCD). Understanding of growth parameters effects on nitrogen incorporation is a prerequisite to repeatably manufacturing of NV^- defects.

After the identification of the stable operation region of the reactor, three samples were grown at 950ºC, 1000ºC, and 1050ºC while holding constant pressure at 290 mbar and feed gas composition to 1216 ppm N:C with 4.17% methane (CH_4) in H_2. High pressure high temperature (HPHT) Sumitomo (100) diamond seeds were used as substrates for these trials. The morphology and growth rate were analyzed to select an optimized substrate temperature during growth. All three samples exhibited smooth step-flow growth and growth rates consistent with the reactor's norm. The optimized substrate temperature was chosen to be 950ºC as the fewest large scale morphological features were observed at this temperature.

Four additional samples were grown on (100) CVD substrates at a constant temperature of 950ºC. The pressure was varied from 250 mbar to 370 mbar in increments of 40 mbar while holding the feed gas composition to 1238 ppm N:C with 4.00% CH_4 in H_2 to observe the effects of plasma density. The four pressure series samples were spectroscopically analyzed using FTIR and UV-Vis spectroscopy. Preliminary results suggest a pressure region where vacancy rich growth dominates. A pressure region with observable graphitic carbon was also identified. Additional growths to verify the spectroscopic results are planned.

* Work supported by the MSU Foundation SPG grant program.

References

[1] Y.Wu, et al., *Nano Lett*., (2021), **21**, 3780-3788.
[2] D. R. Glenn, et al., *Geochem. Geophys. Geosyst.*, **18** (2017), 3254-3267.

II-08. Developing a Shock-Ramp Laser Drive to Extend the Pressure Ranges of the NIF Gbar Platform Single-Shot Hugoniot Measurements*

M. P. Springstead, D. C. Swift, T. Doeppner, C. C. Kuranz, A. Lazicki, M. J. MacDonald

University of Michigan, Ann Arbor, MI (mispring@umich.edu)

Recent Gbar experiments at the National Ignition Facility (NIF) utilize spherically converging shock waves to reach high pressures (>300 Mbar) inside hydrocarbon capsules. Equation of State (EOS) measurements are made as the propagating shock wave drives the hydrocarbon sample along its principal Hugoniot. Further improvements to the Gbar experimental platform are proposed by utilizing a new shock-ramp drive, where the sample is initially shocked then driven with a strong ramp increasing the shock pressure faster than a spherically converging single shock. The goal of the shock-ramp drive is to reach higher pressures within the material sample and increase the ranges of pressures provided in a single experiment. The impacts of the shock-ramp drive would extend the range in which the EOS models can be validated and reduce the number of shots needed to collect Hugoniot data. The shock-ramp drive was designed by modeling the hydrocarbon capsules in the ALE radiation-hydrodynamic code HYDRA. Capsule parameters accounting for the geometry, materials, and laser drive were included in the HYDRA modeling. We present the parameter scan results to illustrate the possible pressure ranges achievable with the shock-ramp drive on the NIF Gbar platform. These findings will be used in upcoming experiments to improve Hugoniot measurements of CH at extreme pressures.

*This work was performed under the auspices of the U.S. Department of Energy by Lawrence Livermore National Laboratory under contract DE-AC52-07NA27344 and supported by Laboratory Directed Research and Development (LDRD) Grant No. 22ERD-005.

II-09. Evanescent-Mode Cavity Resonator-Based Microwave Plasma Jet Technology*

Kazi S. Kabir and Abbas Semnani

The University of Toledo, Toledo, Ohio 43606
(kkabir@rockets.utoledo.edu, abbas.semnani@utoledo.edu)

Plasma Jet is used in medicine, food, water decontamination, lighting, reconfigurable RF electronics, etc. [1]. Although low-power plasma is sufficient for many applications, most current plasma sources are bulky and expensive as they are inefficient in transferring energy to the plasma. Efficient plasma with low power consumption is expected to impact many such applications. Microwave resonant structures can store and enhance EM energy; hence, employing such structure to achieve high-efficiency plasma with low power consumption is possible. The main principle is to utilize resonators that can concentrate the EM fields over a small gap. Then, even with considerably low input power levels, the magnitude of EM fields over those critical gaps can reach the breakdown threshold, resulting in gas breakdown and plasma formation. An EVA cavity resonator is formed by loading a normal cavity by a post at the center. One important consequence of this loading is the electric field concentration in the gap between the resonator post and the top wall. This feature was previously used to implement novel plasma-based high-power microwave limiters and switches.

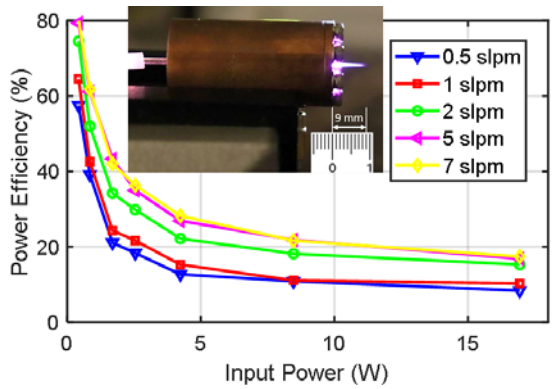

Figure 1 - Power efficiency of the EVA cavity plasma jet for different input powers and gas flow rates.

A novel low-power and highly-efficient atmospheric microwave plasma jet based on evanescent-mode (EVA) cavity technology was introduced in [2]. This design implemented a gas flow mechanism to pass through the EVA critical region and realize a high-efficiency resonant microwave plasma jet. A 2.45 GHz prototype device could operate at power as low as 400 mW with >80% power efficiency and electron density in the range of 10^{15} (cm^{-3}). The maximum jet temperature of the device was approximately 350 K at 10 W input power, showing that the gas temperature is lower than the state-of-the-art plasma jet devices. The results proved the possibility of realizing high-density plasma jets with only milliwatts of power by employing high-*Q* microwave resonant structures. If required, the plasma volume can be extended by either using an array of such jets or scaling the resonator to lower frequencies.

* Work supported by the National Science Foundation under Grant number EECS-2102100.

References

[1] G. Fridman, G. Friedman, A. Gutsol, A. B. Shekhter, V. N. Vasilets, and A. Fridman, "Applied plasma medicine," *Plasma Process. Polym.*, vol. 5, no. 6, pp. 503–533, Aug. 2008.

[2] A. Semnani and K. S. Kabir, "A Highly Efficient Microwave Plasma Jet Based on Evanescent-Mode Cavity Resonator Technology," *IEEE Transactions on Plasma Science*, 2022, doi: 10.1109/TPS.2022.3202509.

II-10. MPACVD Diamond: Growth Conditions and Power Electronics Applications*

Cristian Herrera-Rodriguez and Timothy Grotjohn

Department of Electrical & Computer Engineering, Michigan State Univ., East Lansing, MI 48824, USA
(herrer95@msu.edu)

Single Crystal Diamond (SCD) has remarkable mechanical, thermal, optical, and electrical properties ideal for the application of electronic devices for high power applications. This study looks at using p-type doped epi-layers of diamond for the fabrication of various power electronic devices.

High quality SCD is grown at MSU by Microwave Plasma-Assisted Chemical Vapor Deposition (MPACVD) using a 2.45 GHz microwave resonant cavity system. In this reactor Ultra High Purity (UHP) levels of process gases (H_2, O_2 and CH_4) are used and diborane (B_2H_6) is employed as the boron p-type doping source. A constant temperature of approximately 800ºC and a process pressure of 90 Torr were applied during diamond growth.

High-quality lightly boron doped diamond epilayers are obtained by adding oxygen in the processing gas in amounts of up to 1%. The oxygen addition helps suppress defect formation, etches non-diamond carbon phases, and decreases the surface roughness during the epilayer growth (Fig.1). Achieving smooth p-type doped epi-layers is needed for the fabrication of electronic devices using the bulk conduction of diamond for high power capabilities and temperature stability. Sub-nanometer surface roughness also allows the bonding of different n-type wide-bandgap materials to form heterojunctions with p-type diamond for bipolar devices and thermal management (Fig.2).

This present study demonstrates the control of the growth rate by the oxygen variation in the total gas flow. Also, the incorporation of these p-type diamond epilayers for the fabrication of high power JFETs [1] using a selective growth process. And finally, showing the bonding process of n-type β-Ga_2O_3 [2] and p-type diamond for the fabrication of PN heterojunction diodes.

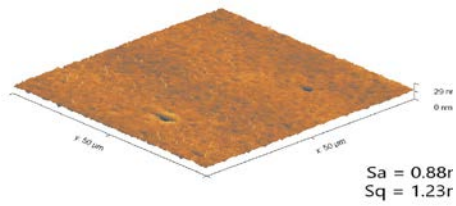

Figure 1 - AFM Measurement after p-epilayer growth (50x50μm area)

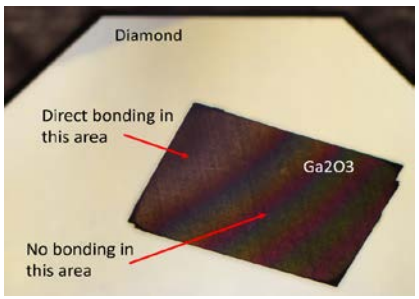

Figure 2 – Optical image of the heterojunction bonding of CVD diamond with β-Ga_2O_3

* Work supported by Ford Motor Co.

References

[1] T. Iwasaki et al., "Diamond semiconductor JFETs by selectively grown n+-diamond side gates for next generation power devices," in 2012 International Electron Devices Meeting, Dec. 2012, p. 7.5.1-7.5.4. doi: 10.1109/IEDM.2012.6478999.

[2] T. Matsumae et al., "Low-temperature direct bonding of β-Ga2O3 and diamond substrates under atmospheric conditions," Appl. Phys. Lett., vol. 116, no. 14, p. 141602, Apr. 2020, doi: 10.1063/5.0002068.

II-11. Reaction Mechanisms for Atmospheric Pressure Plasma Treatment of Organic Molecules in Solution*

Jordyn Polito [a], María J. Herrera Quesada [b], Katharina Stapelmann [b] and Mark J. Kushner [c]

(a) Department of Chemical Engineering, University of Michigan, Ann Arbor, MI 48109-2122 USA, (jopolito@umich.edu)

(b) Department of Nuclear Engineering, North Carolina State University, Raleigh, North Carolina 27607 USA

(c) Department of Electrical Engineering and Computer Science. University of Michigan, Ann Arbor, MI 48109-2122 USA

Small, portable atmospheric pressure plasma jets (APPJs) (e.g. KINpen, COST-jet) are gaining traction in the biomedical community as sources of reactive oxygen and nitrogen species (RONS) for bactericidal applications. Plasma-produced RONS solvate into solution and are thought to interact with amino acids located on cell walls to irreversibly change the functionality of cells in solution. To further understand this phenomena, fundamental investigations utilizing APPJs have focused on plasma-liquid interactions of RONS with simple biologically-relevant amino acids (e.g., cysteine) in solution. Experimental studies have shown RONS are depleted in reactions with simple amino acids in solution, producing oxidation products that are similar to those formed by treatment of organic molecules with gas-phase plasmas [1]. Reaction mechanisms for plasma-liquid interactions are generally available for solutions that do not contain organic molecules and materials. Development of these mechanisms could provide insight for biological applications.

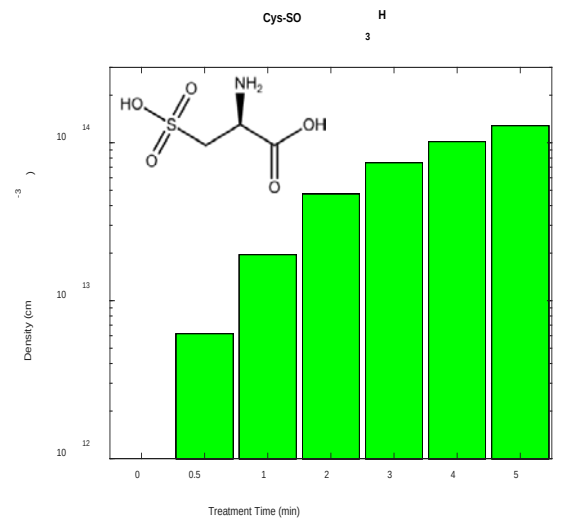

Figure 1 – Density of sulfonic acid (cysteine oxidation product) after 5 minutes treatment by $He/O_2/N_2$, 5 W, COST-jet produced APPJ.

In this work we develop a reaction mechanism for the computational investigation of APPJ treatment of cysteine in water. A global plasma chemistry model adapted for plasma-liquid interactions was used to investigate the effects of plasma activated oxidizing (e.g., O, OH) species on the final oxidation states of cysteine in solution. The interactions of these RONS with the cysteine molecule will be discussed and compared to experiments.

* Work supported by the US NSF, DOE Fusion Energy Sciences and the Army Research Office MURI Program.

References

[1] K. Stapelmann et al., J. Phys. D Appl. Phys. 54, 434003 (2021).

II-12. Faraday Rotation Imaging of X-Pinch Implosion Dynamics

G. V. Dowhan [a], J. M. Chen [a], A. P. Shah [a], B. J. Sporer [a], N. M. Jordan [a], S. N. Bland [b], S. V. Lebedev [b], R. A. Smith [b], L. Suttle [b], S. A. Pikuz [c], and R. D. McBride [a]

(a) University of Michigan (dowhan@umich.edu)
(b) Imperial College London
(c) Lebedev Physical Institute

X-pinches, formed by driving intense current through the crossing of 2 or more wires, provide an excellent platform for the study of "micro-pinches" due to their propensity to generate a single micro-pinch at a predetermined location in space (i.e., where the wires cross) [1,2]. Ideally, micro-pinches are areas of run-away compression to very small radii (~1 µm) leading to pressures on the order of ~1 Gbar for currents on the order of ~0.1 MA. However, the fraction of the total current that is driven through the dense micro-pinch plasma at small radii versus that being shunted through the surrounding coronal plasma at larger radii is not well known. To allow for the study of micro-pinches and their current distribution, experiments have been run on the 1-MA MAIZE facility utilizing a Faraday rotation imaging diagnostic (1064 nm) [3] designed with the primary goal of achieving high magnification measurements of the current distribution near the pinch. The diagnostic can achieve variable magnifications of 1-10x (or more) with a spatial resolution of approximately 35 µm, which is then useful to allow radial measurements of the azimuthal magnetic field distribution within the ~100-µm-scale neck-down region surrounding the X-pinch during its implosion. Combined with the corresponding interferogram providing the radial density distribution, the measured rotation can be used to diagnose the delivery of the driver current to the micro-pinch plasma as it approaches minimal radius, and therefore the overall limit of the magnetic drive pressure.

*This work was supported by the DOE Early Career Research Program under Grant DE-SC0020239 and by the NNSA SSAP under Cooperative Agreement DE-NA0003764.

References

[1] S. A. Pikuz, T. A. Shelkovenko, and D. A. Hammer, Plasma Physics Reports. **41**, 291 (2015).
[2] S. A. Pikuz, T. A. Shelkovenko, and D. A. Hammer, Plasma Physics Reports. **41**, 445 (2015).
[3] G. F. Swadling et al., Review of Science Instruments, **85**, 11E502 (2014)

II-13. Inductive Probing in a Rotating Magnetic Field Thruster*

Christopher L. Sercel, Tate M. Gill and Benjamin A. Jorns

University of Michigan, Department of Aerospace Engineering (csercel@gmail.com)

The Rotating Magnetic Field (RMF) thruster is an example of an inductive pulsed plasma thruster (IPPT) which employs a rotating magnetic field to induce an azimuthal current in a plasma. This current interacts with the radial component of a stead bias magnetic field, resulting in an axial body force on the plasma, ejecting the propellant in a slug and generating impulse. As an IPPT, the RMF thruster is highly throttleable, in-situ resource utilization (ISRU) compatible, and boasts very high specific power.[1] Unlike other IPPTs, the RMF thruster has the added benefit that, under nominal operation, driven plasma current is proportional to the frequency rather than the magnitude of the driving magnetic field, allowing for significantly relaxed power supply requirements and better power supply longevity.[2]

Initial performance measurements of the RMF thruster show poor performance, despite coupling relatively large amounts of energy into the plasma (up to 700 J/mg), suggesting the current drive or acceleration mechanism may not be functioning as anticipated.[3] Further, performance was seen to improve with increased RMF field strength despite Jones and Hugrass penetration limits having been met, which should ensure that driven current depends only on RMF frequency.[4] In light of these uncertainties regarding the current drive mechanism, there is a pressing need for time-resolved azimuthal current density measurements throughout the thruster and plume.

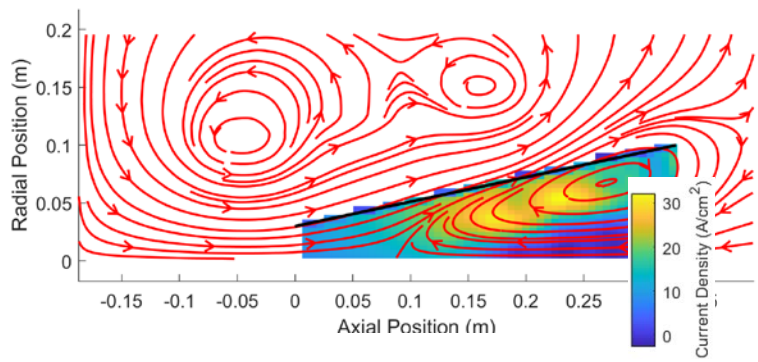

Figure 1 – Magnetic field streamlines overlaid on a current density plot of the RMF thruster, 70 us into a 125 us pulse.

To address this, inductive probing techniques were used to produce a 2-dimensional map of both the radial and axial components of the induced magnetic field over the course of the pulse. Through Ampere's law, this directly gives the local azimuthal current density as well. By combining the current density and magnetic field strengths, Lorentz forces throughout the plasma can be estimated and compared to thrust stand measurement.

*Work supported by NSTRF Grant # 80NSSC18K1190 (Sercel) and NSTGRO Grant # 80NSSC20K1168 (Gill).

References

[1] Polzin, K., Martin, A., Little, J., Promislow, C., Jorns, B., and Woods, J., "State-of-the-Art and Advancement Paths for Inductive Pulsed Plasma Thrusters," Aerospace, Vol. 7, No. 8, 2020, p. 105.

[2] Blevin, H. A., and Thonemann, P. C., "Plasma confinement using an alternating magnetic field," Nuclear Fusion Supplement,Part 1, 1962, p. 55.

[3] Sercel, C. L., Gill, T., Woods, J. M., and Jorns, B., "Performance Measurements of a 5 kW-Class Rotating Magnetic FieldThruster," AIAA Propulsion and Energy 2021 Forum, 2021, p. 3384.

[4] Jones, I. R., and Hugrass, W. N., "Steady-state solutions for the penetration of a rotating magnetic field into a plasma column," Journal of Plasma Physics, Vol. 26, No. 3, 1981, pp. 441–453.

II-14. Preliminary Results for Experiment at WiPPL*

Khalil Bryant [a], Rachel Young [a], Joseph Ray Olson [b], Cary Forest [b] and Carolyn Kuranz [b]

(a) University of Michigan, Ann Arbor (kalelb@umich.edu)
(b) University of Wisconsin, Madison

The Sun, being an active star, undergoes eruptions of magnetic fields and charged particles that reach the Earth and cause the aurora near the poles.
Some eruptions may be more powerful than others, resulting in an Interplanetary Coronal Mass Ejection (ICME) that can cause major damage to our modern electrical systems without warning.
We want to form a better understanding of how the ICMEs interact to create a more predictive model for them to more effectively defend our systems from a potentially devastating ICME.
For this project, we use the Big Red Ball (BRB) facility at the Wisconsin Plasma Physics Laboratory (WiPPL). The BRB is a 3-meter diameter plasma confinement system equipped with around 200 ports for diagnostic acess. Using the BRB, we affirmatively answer the question, "Can we create a scaled analog of an ICME in a laboratory environment?" My presentation will show some preliminary data from this experiment and provide some insight to the methods of analysis.

* This work is funded by the US Department of Energy Office of Science Fusion Energy Sciences under award DE-SC0021288 and is partially supported by the DoE collaborative research facility WiPPL under award DE-SC0018266.

II-15. Beryllium Probe Neutron Diagnostic for a Gas-Puff Z-Pinch Neutron Source on a 1-MA, 100-ns Linear Transformer Driver*

D.E. White [a], A.P. Shah [b], and R. D. McBride [c]

(a) Electrical Engineering and Computer Science, University of Michigan (dejwhite@umich.edu)
(b) Applied Physics Program, University of Michigan (akashah@umich.edu)
(c) Nuclear Engineering and Radiological Sciences, University of Michigan (mcbrider@umich.edu)

The purpose of this study is to develop a diagnostic suite for studying neutron production in gas-puff z-pinch experiments on the Michigan Accelerator for Inductive Z-Pinch Experiments (MAIZE). Of particular interest is measuring neutron yields from deuterium-deuterium (DD) fusion reactions. MAIZE is a 1-MA, 0.1-TW, 100-ns Linear Transformer Driver (LTD) [1]. The intense current pulse generated by MAIZE is used to implode cylindrical plasmas, with applications in inertial confinement fusion, x-ray source development, material properties, and laboratory astrophysics [2]. A gas-puff z-pinch is a specific load configuration where an annular column of gas is ionized and pinched by the magnetic Lorentz force, $\mathbf{J} \times \mathbf{B}$. The gas puff is injected into the load region on MAIZE by a nozzle and fast-valve assembly. The injected column of gas becomes the load, completing the circuit by bridging MAIZE's anode-cathode gap. Neutron production has been demonstrated recently on MAIZE [3], but accurate measurements of the neutron yield are needed. One way to obtain accurate yield measurements is through the use of scintillation techniques, where ionizing radiation is detected by the light produced in a scintillator material. Most scintillation materials convert the kinetic energy of charged particles into detectable light, where the conversion is linear, and the light yield is proportional to the deposited energy over a wide range. The decay time of the luminescence is short where fast signal pulses are generated [4]. The diagnostic developed for this study is comprised of a beryllium (Be) probe detector, with Be rods in a scintillating material, and a photomultiplier tube (PMT), all within a shared housing. We also used a suite of instrumentation from ORTEC, including ORTEC's Minibin and Power Supply, 5-kV Detector Bias Supply, Constant-Fraction Discriminator, and EASY-MCS Multichannel Scaler. In this presentation, the scientific background and experimental setup of the diagnostic will be discussed. Of particular importance is the configuration of the Be detector and the procedure used to analyze and configure the Multichannel Scaler data for neutron yields [5].

* This work was supported by the DOE-NNSA through the SSAA Program under Cooperative Agreement No. DE-NA0003764.

References

[1] R. M. Gilgenbach et al., "MAIZE: A 1 MA LTD-driven Z-pinch at the University of Michigan," in Proc. AIP Conf., Jan. 2009, vol. 1088, no. 1, pp. 259–262, doi: 10.1063/1.3079742.
[2] R. D. McBride et al., "A Primer on Pulsed Power and Linear Transformer Drivers for High Energy Density Physics Applications", IEEE Trans. Plasma Sci. vol. 46, pp. 3928–3967 (2018), doi: 10.1109/TPS.2018.2870099.
[3] A. P. Shah et al., "Development of a Gas-Puff Z-Pinch Neutron Source for the 1-MA, 100-ns MAIZE Linear Transformer Driver", manuscript in preparation (2021).
[4] G. Knoll, "Radiation Detection and Measurement", 4th ed. John Wiley & Sons (2010).
[5] C. L. Ruiz et al., "Novel beryllium-scintillator, neutron-fluence detector for magnetized liner inertial fusion experiments," Phys. Rev. Accel. Beams, vol. 22, no. 4, p. 042901, Apr. 2019, doi: 10.1103/PhysRevAccelBeams.22.042901.

III-01. Conservative Structure Functions via Multispecies BGK Kinetic Equation

Thomas Chuna [a], Michael Murillo [b]

(a) Michigan State University, Dept. of Physics and Astronomy (chunatho@msu.edu)
(b) Michigan State University, Dept. of Computational Mathematics, Science, and Engineering (murillom@msu.edu)

In the literature, response functions are known for the quantum and classical Fermi gas. Originally it was the Vlasov function, then Mermin published the much celebrated number conserving response function [1]. Many decades later, Atwal and Ashcroft [2] extended Mermin's method to conserve the first three moments (mass, momentum, energy). However, preceding Mermin was Bhatnagar, Gross, and Krook [3] who developed the celebrated BGK collisional model. This collisional model is a relaxation model very similar to Mermin's, but it conserves (mass, momentum, energy) like Atwal and Ashcroft. It is shown in this paper that both Mermin's electron gas response function and Atwal and Ashcroft's response function can be produced as a limiting case of the single species BGK relaxation model. Furthermore, The present authors argue that Mermin did not complete his own response function. Mermin's response function can be trivially extended to include momentum conservation. The *completed Mermin* response function is extended from single species to multiple species using the recently developed Multispecies BGK model [4].

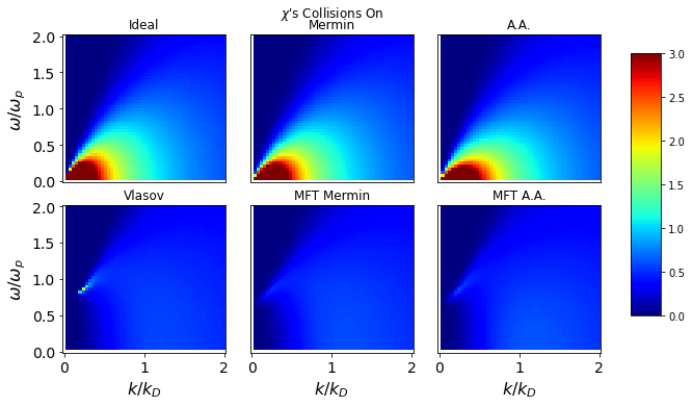

Figure 1 – Top row contains plots of the Ideal gas, Mermin, and Atwal Ashcroft structure functions. Bottom row contains the mean field corrected (i.e. Vlasov) version of these response functions.

References

[1] N. D. Mermin Phys. Rev. B **1**, 2362 (1970).
[2] G. S. Atwal and N. W. Ashcroft, Phys. Rev. B **65**, 115109 (2002).
[3] P. L. Bhatnagar and E. P. Gross and M. Krook, Phys. Rev. **94** (1954).
[4] Haack, Hauck, Murillo, J. Stat. Phys. **168**, 826 (2017).

III-02. Investigation of the Interaction Between Non-Thermal Plasma Activated Nitrogen and Metal Surfaces*

Garam Lee [a], Chang Yan [a], William F. Schneider [a,b], David B. Go [a,c], and Casey P. O'Brien [a]

(a) Department of Chemical and Biomolecular Engineering, University of Notre Dame, Notre Dame, IN 46556 (glee4@nd.edu)
(b) Department of Chemistry and Biochemistry, University of Notre Dame, Notre Dame, IN 46556
(c) Department of Aerospace and Mechanical Engineering, University of Notre Dame, Notre Dame, IN 46556

There has been a growing interest in the integration of conventional heterogeneous catalysis with reactive chemical environments induced by non-thermal plasmas (NTPs) to promote catalytic activities and even novel chemical transformations that neither plasma nor catalysis could deliver individually. Despite the promise, the influence of NTP activation of molecules on elementary surface processes such as adsorption, surface reaction, and desorption at a catalytic surface remains primitive. Here, we report observations of the adsorbed nitrogen species from the interaction between NTP-activated nitrogen (N_2) and polycrystalline Ni, Pd, Cu, Ag, and Au surfaces using a newly-designed multi-modal spectroscopic tool that combines polarization-modulation infrared reflection-absorption spectroscopy (PM-IRAS), mass spectrometry (MS), and optical emission spectroscopy (OES), combined with density functional theory (DFT) models to rationalize those observations. Observations and models indicate that NTP activation provides access to metastable surface nitrogen species that are inaccessible thermally. Taken together, the results shed light on the role of NTP activation in the promotion of surface reactions.

* This work is based on support from the National Energy Technology Laboratory (NETL) under Award No. DE-FE0031862.

III-03. Plasma Parameter Scaling at High Powers for a Magnetically Shielded Hall Thruster Operating on Krypton

Leanne L. Su, Thomas A. Marks and Benjamin A. Jorns

University of Michigan (leannesu@umich.edu)

Hall thrusters are a mature electric propulsion technology with the potential to scale to the 100-kW range, which may enable crewed deep space travel. Magnetic shielding, a magnetic field topology that reduces thruster erosion, has extended the lifetimes of these devices, but the internal plasma properties of the thrusters differ from the traditional "unshielded" configuration [1,2]. Additionally, while the traditional propellant of choice is xenon for its high mass and low ionization energy, the price of xenon has increased rapidly in recent years. Krypton is one possible alternate propellant, but its performance—particularly on shielded thrusters—is poor compared to xenon [3]. There is therefore an apparent need to understand the performance of magnetically shielded Hall thrusters operating on krypton and how they scale to higher powers. This poster will present results from a multifluid simulation of a Hall thruster that have been calibrated with performance metrics such as thrust, discharge current, and ion velocity profiles [4,5]. These simulations are then used to determine how various internal plasma parameters scale with both increasing current and voltage. The results are discussed in context of how they may impact thruster efficiencies at various operating conditions.

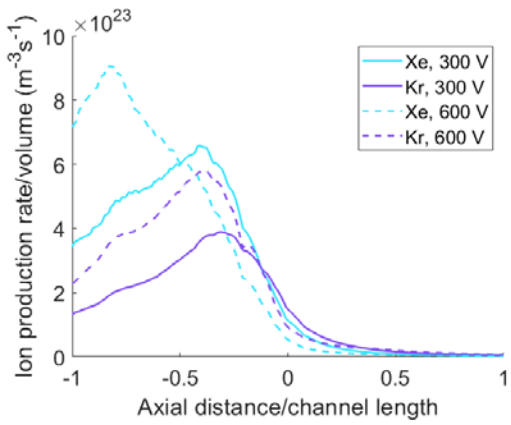

Figure 1 – Rate of ion production per unit volume for xenon and krypton at 300 V and 600 V determined from calibrated Hall2De simulations. The 0 on the x axis indicates the exit plane of the channel, while -1 indicates the position of the anode. [5]

References

[1] I. G. Mikellides, I. Katz, R. R. Hofer, and D. M. Goebel, J. Appl. Phys. **115,** 043303 (2014).
[2] R. R. Hofer, D.M. Goebel, I. G. Mikellides, and I. Katz, J. Appl. Phys. **115,** 043304 (2014).
[3] L. L. Su and B. A. Jorns, J. Appl. Phys. **130,** 163306 (2021).
[4] I. G. Mikellides and I. Katz, Phys. Rev. E., **86,** 046703 (2012).
[5] L. L. Su, T. A. Marks, and B. A. Jorns, International Electric Propulsion Conference (2022).

III-04. Mitigation of Stray Light for Low-Temperature Thomson Scattering in DIII-D*

Parker J. Roberts [a], Fenton Glass [b], and Benjamin Jorns [a]

(a) University of Michigan (pjrob@umich.edu)
(b) General Atomics (fglass@fusion.gat.com)

Thomson scattering, the elastic scattering of photons from free electrons, is a key plasma diagnostic for thermonuclear fusion research due to its ability to provide spatiotemporally resolved measurements of the electron density and temperature [1]. Due to the high intensity of laser light sources necessary for this diagnostic, stray light from reflected laser photons can overwhelm the relatively small Thomson scattering signal. The Thomson scattering diagnostic at the DIII-D National Fusion Facility uses an array of 7-channel polychromators with optical interference filters in order to detect the Thomson spectrum [2]. This work considers design modifications to these polychromators in order to reduce the intensity of stray light which bleeds through the filters and obscures the Thomson photons through optimizing the light-strike order of optical filters. Ultra-narrow bandpass filters are implemented in series as a stray light rejection stage before spectrum detection, in which the filters pass 1064-nm YAG laser light out of the device to reduce the disproportionate intensity of these photons relative to the Thomson signal. This redesigned polychromator is characterized experimentally, through both steady-state scans with low-intensity monochromatic light and a full laser shot in the tokamak.

It is found that a pre-filtering stage consisting of 2 stray light filters in parallel is able to reduce the intensity of laser photons which bleed through the low-temperature detection channels by a factor of 10. This reduction in stray light signal decreases the sometimes critical error in low-temperature measurements with high stray light, such as those taken in the divertor region, where the convolution of the signal of interest with the complicated and time-varying reflected signal can add significant uncertainty to the measurement.

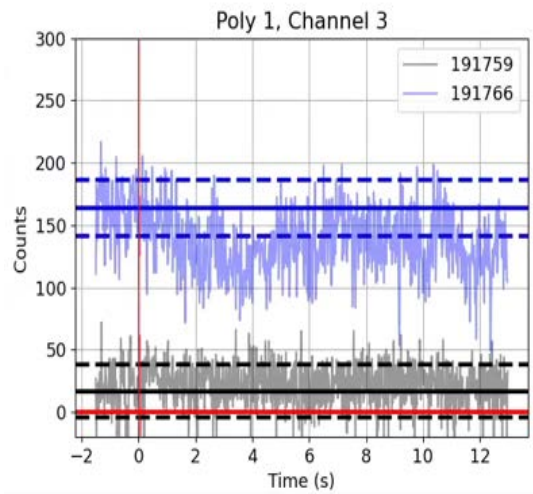

Figure 1 – Reduction of stray light passing through a 1062-nm detector at 1064 nm, the YAG laser wavelength. The blue and gray signals are the stray light over time in standard and modified polychromators, respectively.

* Work supported by a NASA Space Technology Graduate Research Opportunity.

References

[1] Sheffield, J., Froula, D., Glenzer, S. H., & Luhmann Jr, N. C. (2010). *Plasma scattering of electromagnetic radiation: theory and measurement techniques*. Academic press.

[2] Carlstrom, T. N., DeBoo, J. C., Evanko, R., Greenfield, C. M., Hsieh, C. L., Snider, R. T., & Trost, P. (1990). A compact, low cost, seven channel polychromator for Thomson scattering measurements. *Review of Scientific Instruments*, *61*(10), 2858–2860. https://doi.org/10.1063/1.1141806.

III-05. Low Bias Frequencies in ICP Reactors for High Aspect Ratio Plasma Etching*

Evan Litch [a], Hyunjae Lee [b], Sang Ki Nam [b] and Mark J. Kushner [a]

(a) University of Michigan, Ann Arbor, MI 48109-2122, USA (elitch@umich.edu)

(b) Mechatronics Research, Samsung Electronics Co., Ltd., 1-1 Samsungjeonja-ro, Hwaseong-si, Gyeonggi-do 18448, Republic of Korea

Semiconductor processing employs inductively plasmas (ICPs) with large substrate biases to fabricate features with high aspect ratios (HAR) for the production of high-density memory. To maintain critical dimensions of these HAR structures, ion energy and angular distributions (IEADs) must have increasingly high energies and narrow angular distributions. To achieve these goals, substrate biases with progressively lower frequencies are being used. Since lower frequencies are not efficient at heating electrons and plasma production, these systems are typically ICPs where the wave heating sustains the plasma. The trend towards lower frequencies is intended to extend the maximum ion energy to fully that of the sum of the RF amplitude and DC bias, while narrowing the IEAD. However, these lower frequencies also produce nearly quasi-steady state conditions, which affects sheath thickness and flux uniformity, and charging of adjacent surfaces.

In this work, results from a computational investigation of ICPs using very low bias frequencies will be discussed. The simulations, conducted with the Hybrid Plasma Equipment Model (HPEM) in tandem with the Monte Carlo Feature Profile Model (MCFPM), investigated a single test system – an ICP sustained in $Ar/Cl_2/O_2$ ICPs. IEADs, uniformity of fluxes to the wafer and sheath structure for these systems for substrate biases as low as 250 kHz will be discussed.

* Work was supported by Samsung Electronics Co. and the US National Science Foundation (2009219).

III-06. Characterizing Hot Electrons in Ensemble PIC Simulations of High-intensity, Laser-plasma Interactions with Machine Learning

Andre F. Antoine [a,b], Blagoje Z. Djordjevic [b] and Derek A. Mariscal [b]

(a) University of Michigan (aantoine@umich.edu)
(b) Lawrence Livermore National Laboratory (djordjevic3@llnl.gov, mariscal2@llnl.gov)

In the interaction of high-intensity lasers with over-dense plasmas, the hot electron population dictates system dynamics, driving ion acceleration and x-ray generation, and fast ignition, for example. The primary method for modeling these systems are particle-in-cell simulations (PIC), where macroparticles approximate the kinetics of a distribution of particles. A problem shared with experiments, PIC simulations are inherently noisy given the statistical nature of the algorithm, particularly at lower fidelities. Individual electron energy distributions are easily analyzed with expert examination, but 'by hand' analysis is impractical for the hundreds of thousands of case examples produced by ensemble simulations, and this is exacerbated by noisy data. In this work, data from an ensemble of PIC simulations is analyzed and quantified using machine learning (ML) techniques to extract the hot electron temperature and other physical parameters more reliably. We present the dependency of the hot electron temperature and other electron sheath properties on various input parameters such as laser intensity and pulse length across a wide parameter space (~10^18-10^21 W/cm^2, 30-500 fs).

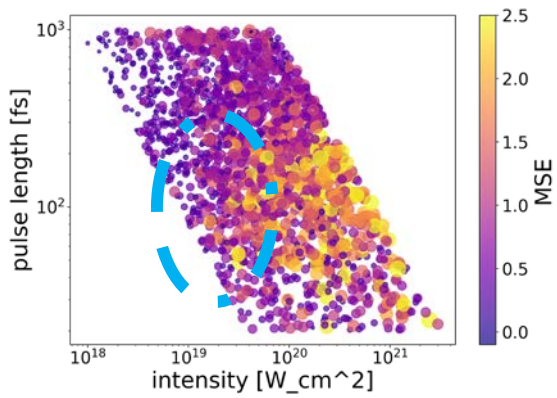

Figure 1 - The mean squared error of naive fits of electron energy distributions plotted against proxys for experimental input, Laser Intensity [W/cm^2] and Pulse Length [fs].

* This work was completed under the auspices of the U.S. Department of Energy by Lawrence Livermore National Laboratory under contract DE-AC52-07NA27344 and funded by DOE-SC FWP 1722 with funding support from the Laboratory Directed Research and Development Program under tracking codes 20-ERD-048 and 22-ERR-022 and the LLNL HED Center.

III-07. Quantum Pathways Interference in Photoemission from Biased Metal Surfaces Induced by Two-color Lasers*

Yang Zhou and Peng Zhang

Department of Electrical and Computer Engineering, Michigan State University, East Lansing, Michigan 48824-1226, USA (pz@egr.msu.edu)

Coherent control of quantum systems relies on the manipulation of quantum interference via external fields such as laser pulses. Two-color coherent control of photoemission from nanotips has drawn intense attention for its capability of characterizing and manipulating electron dynamics in ultrashort temporal and spatial scales, and for the new opportunities in applications such as time-resolved electron microscopy, and emerging nanophotonic and nanoelectronic devices. It is of high interest to analyze the quantum pathway interference using exact quantum theory to study the underlying physics and therefore to provide better quantum coherent control of photoemission from metal surfaces.

Here, we analyze the quantum pathways interference in two-color laser induced photoemission, using an exact analytical solution of the time-dependent Schrödinger equation [1-3]. The theory includes contributions from all possible quantum pathways and interferences among them. Effects of laser and dc bias fields on the weight of each pathway and the interference terms are studied. Increasing the intensity ratio of the second harmonic to fundamental lasers results in more contribution from multicolor pathway (absorption of both ω- and 2ω-photons) and the single-color pathway of absorption of 2ω-photons, and therefore stronger interference between them and increased visibility >95%. Increasing bias voltages shifts the dominant emission with fewer photon absorption, which sequentially decreases the interference between the ω- and the 2ω-pathways, and between single-color and multicolor pathways. Our study provides insights into the underlying physics of coherent control of two-color photoemission.

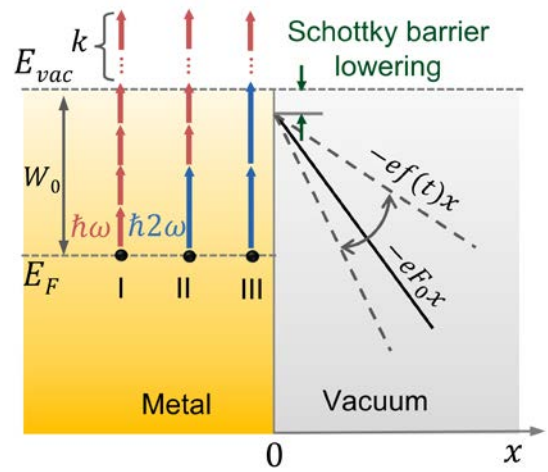

Figure 1 – Energy diagram for photoemission from a metal surface induced by two-color laser fields $f(t)=F_1\cos(\omega t)+F_2\cos(2\omega t+\theta)$ under a dc field F_0. Red and blue arrows depict quantum pathways model, with I: absorption of (4+k) ω-photons (red arrow); II: absorption of (2+k) ω-photons and 1 (2ω)-photons (blue arrow); III: absorption of 2 (2ω)-photons and k ω-photons.

* Work supported by AFOSR YIP Grant No. FA9550-18-1-0061 and ONR YIP Grant No. N00014-20-1-2681.

References

[1] Y. Luo and P. Zhang, Phys. Rev. B 98, 165442 (2018).
[2] Y. Luo and P. Zhang, Phys. Rev. Applied 12, 044056 (2019).
[3] Y. Zhou and P. Zhang, Phys. Rev. B 106, 085402 (2022).

III-08. Photoionization Front Laboratory Experiments at the OMEGA Laser Facility*

K. V. Kelso [a], H. J. LeFevre [a], S. R. Klein [a], P. A. Keiter [a,b], W. J. Gray [a], J. S. Davis [a], R. P. Drake [a], C. C. Kuranz [a]

(a) University of Michigan, Center for Laboratory Astrophysics, Ann Arbor, Michigan, 48105, USA (kkelso@umich.edu)
(b) Los Alamos National Laboratory, Los Alamos, New Mexico, 87544, USA

Photoionization fronts are meaningful drivers of transformation for astrophysical phenomena. Generating sufficiently intense x-rays in laboratory experiments has been a difficult challenge. We attempt to create an environment relevant to astrophysical systems in which intense photon fluxes drive ionization and dynamics. Experiments at the OMEGA Laser Facility can create relevant photoionization conditions. One can generate a backlighter X-ray source through the ablation of an 860 micron diameter spherical nickel lined CH capsule. A laser irradiated gold foil generates an intense, thermal X-ray source (80-90 eV) which propagates into a gas cell filled with argon for the investigation of the Kα-absorption edge (3.203 keV). We present the preliminary results from an analytical study of the cold argon gas K-shell edge line absorption, characterized with a streak x-ray spectrometer using an RbAP crystal. We measured the K-edge of X-ray absorption spectra of argon gas using 2-4keV continuum photon energy from the capsule implosion.

* This work is funded by the U.S. Department of Energy NNSA Center of Excellence under cooperative agreement number DE-NA0003869.

III-09. Controllable Electron Injection for Laser Wakefield Acceleration Using Co-Propagating Laser Pulses*

Nicholas Ernst, Alec Thomas and Karl Krushelnick

University of Michigan, Ann Arbor (npegyf@umich.edu)

We introduce a novel method of controlled electron injection for Laser Wakefield Acceleration (LWFA) [1] operating in the high-intensity “bubble” regime. In this scheme, a fraction of a high-intensity (>10^{18} W/cm^2) "driver" pulse is diverted and compressed into a low power, few-cycle "satellite" pulse co-propagating alongside the driver. This satellite is tightly focused off-axis where it acts to perturb bubble formation and drive an asymmetric plasma wave before stabilizing on-axis. Using the plasma as a nonlinear coupling media between the two pulse [2] allows for manipulation of the particle Hamiltonian, creating a trigger to overcome the wave-breaking injection threshold and lead to efficient particle trapping and acceleration. 2D OSIRIS [3] and quasi-3D FBPIC Particle-in-Cell (PIC) simulations support this concept, demonstrating that systematic investigation of the two-beam parameter space (e.g. temporal delay, beam displacement, etc.) leads to controllable variance in the electron beam phase space. Results indicate this method could be used to induce self-injection in wakefields both at plasma densities and driving laser intensities well below theoretical predictions. The results show promise for an all-optical route to high charge, mono-energetic particle acceleration to GeV energies or enhancement of electron betatron radiation through independent tuning of the satellite pulse.

* This work is supported in part by the U.S Department of Energy Office of Science

References

[1] E. Esarey, C. B. Schroeder, and W. P. Leemans, Rev. Mod. Phys. 81, 1229 (2009).
[2] C. Ren et al, Physics Of Plasma 9, 2354 (2002).
[3] R A Fonseca *et al*, *Plasma Phys. Control. Fusion* 50 124034 (2008).

III-10. Evidence of Gas Phase Nucleation of Nano Diamond Through the Analysis of Activation Energy

Tanvi Nikhar [a], Shengyuan Bai [b] and Sergey V. Baryshev [a]

(a) Department of Electrical and Computer Engineering, Michigan State University, 428 S. Shaw Ln., East Lansing, MI 48824, USA (nikharta@msu.edu)

(b) Department of Chemical Engineering and Materials Science, Michigan State University, 428 S. Shaw Ln., East Lansing, MI 48824, USA

The mechanism of ballas like nano diamond formation still remains elusive, and this work attempts to analyze its formation in the framework of activation energy (E_a). Nano diamond thin films were grown from $H_2/CH_4/N_2$ plasma in a 2.45 GHz chemical vapor deposition system.[1] The E_a is calculated using the Arrhenius equation corresponding to the thickness growth rate, mass growth rate, and renucleation rate, using substrate temperature (~ 1000 − 1300 K) in all the calculations.

While the calculated values match with the E_a for nano diamond formation throughout the literature, these values of ~10 kcal/mol are far off compared to ~50 kcal/mol for standard single crystal diamond (SCD) formation shown in Figure 1, concluding thus far, that the energetics and processes involved are different. To further elaborate this, we modified the substrate preparation and sample collection method while keeping the growth parameters constant: un-seeded substrates were used that were physically separated from the plasma by a metal stub with a pinhole for sample collection. Electron microscopy and Raman spectroscopy of the collected sample found that nano diamond self nucleates in the plasma and flows to the substrate which acts as a mere collection plate.

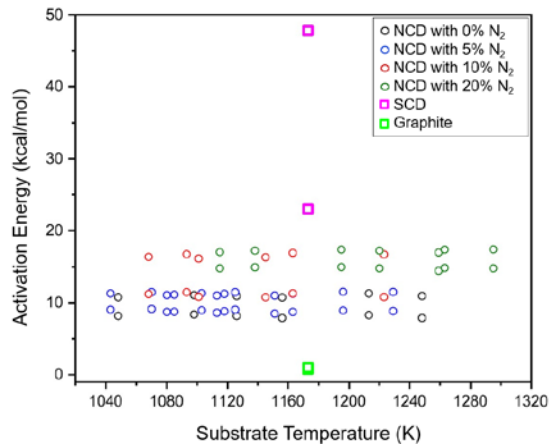

Figure 1 - Activation energies corresponding to the thickness growth rates of nano crystalline diamond (NCD) films grown with different nitrogen contents compared with the activation energy of formation of single crystal diamond (SCD) and pure graphite.

The E_a values for all the nano diamond films are now re-calculated using the approximated gas temperature (~ 2000 − 3000 K), giving values closer to SCD formation. It suggests that the formation process for nano diamond and SCD could be the same, but the formation happens in the gas phase for nano diamond and directly on the substrate for SCD.

References

[1] T. Nikhar, R. Rechenberg, M. F. Becker and S. V. Baryshev, J. Appl. Phys. **128**, 235305 (2020).

III-11. Numerical Simulation of the Hollow Cathode Plasma Discharge Using the Continuum-kinetic Method in 2D-2V*

Moises A. Enriquez [a,b] and Michael D. Campanell [b]

(a) The University of Michigan (mosiesae@umich.edu)
(b) Lawrence Livermore National Laboratory (campanell1@llnl.gov)

Plasma sheaths inside a hollow cathode (HC) shown in Fig. 1 are investigated numerically using a continuum-kinetic method [1]. This approach allows for a self-consistent model that tracks the evolution of the distribution functions for both ions and electrons without the use of fluid assumptions. Ionization, charge-exchange, and thermalization collisions have been implemented to study the effects the sheaths have on the plasma discharge. A fluid model for the neutral species has been implemented to complement the spatially and kinetically dependent collisional processes. The primary motivation of this work is to establish the feasibility of non-classical sheaths that are found near emissive surfaces inside of a HC. These structures may have a direct impact on the performance and operation of the HC due to changes in thermal transport, erosion due to ion bombardment, and thermionic emission due to plasma-induced surface heating [2,3]. The resulting simulations will represent, to the authors' best knowledge, the first cleanly-resolved sheath structures inside an HC using a collisional kinetic model in 2D-2V.

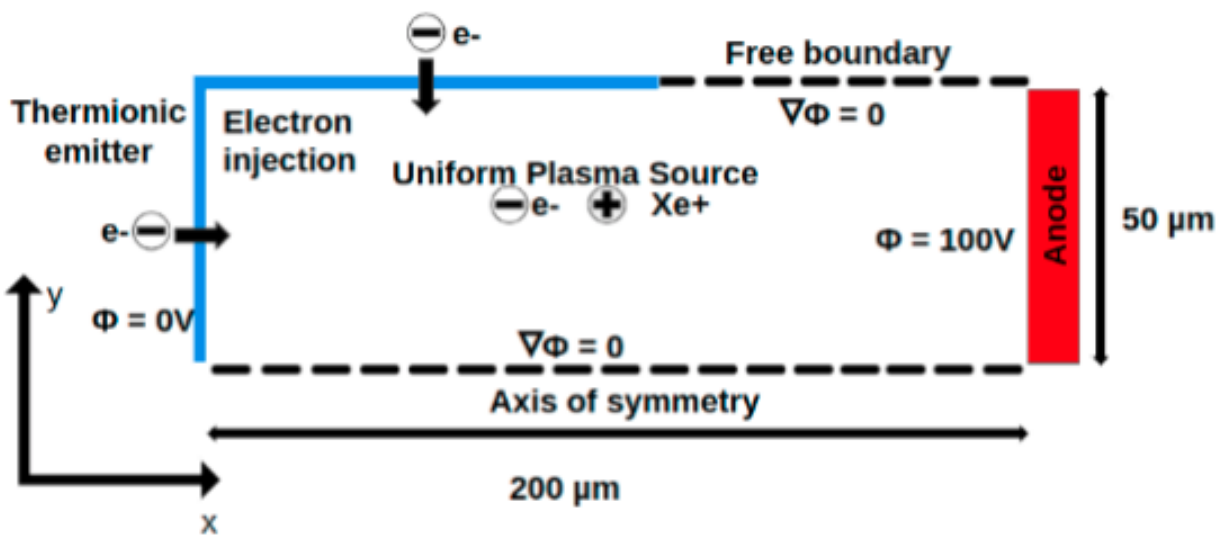

Fig. 1 Schematic of the simulation domain

* This work was performed under the auspices of the U.S. Department of Energy by Lawrence Livermore National Laboratory (LLNL) under Contract No. DE-AC52-07NA27344. This research used resources of the National Energy Research Scientific Computing Center (NERSC), a U.S. Department of Energy Office of Science User Facility operated under Contract No. DE-AC02-05CH11231.

References

[1] G. Johnson et al., PSST. **30**, No. 01 (2021).
[2] D. Levko et al., Phys. Of Plasmas. **20**, No. 08 (2013).
[3] D. Cao et al., Phys. Of Plasmas. **25**, No. 10 (2018).

III-12. Exploding Thin Liner Experiment on MAIZE*

J. M. Chen [a], G. V. Dowhan [a], A. P. Shah [a], B. J. Sporer [a], D. A. Yager-Elorriaga [b] and R. D. McBride [a]

(a) Nuclear Engineering and Radiological Sciences, University of Michigan, Ann Arbor, MI 48109, USA (joech@umich.edu)
(b) Sandia National Laboratories, Albuquerque, NM 87185, USA

One of the major concerns in magnetized liner inertial fusion (MagLIF) experiments on Z is the development of the magneto Rayleigh-Taylor (MRT) instability, which causes degradation to the confinement of thermonuclear fuel. MRT is observed to create helical plasma striations when an axial magnetic field is pre-embedded along the liner with external coils. A hypothesis for the origin of this so-called helical instability is from magnetic flux compression of a low-density plasma (LDP) around the liner originating from the high current densities on the transmission lines leading up to the liner. To study this hypothesis, we are developing a suite of laser-based diagnostics that will provide temporally resolved images as well as density measurements capable of studying LDPs and their interaction onto an imploding liner. The two laser diagnostics under development are a laser schlieren refractometer [2] and a laser interferometer system, both with a 532-nm probe beam from a Nd:YAG laser. We present the development of the optical diagnostic suite along with an initial exploding thin liner experiment results on the University of Michigan's MAIZE facility, a 1-MA class linear transformer driver.

* Work supported by SNL LDRD Project No. 22-0671. SNL is managed and operated by NTESS under DOE NNSA contract DE-NA0003525.

References

[1] D. Yager-Elorriaga et al., "An overview of magneto-inertial fusion on the Z Machine at Sandia National Laboratories," Nuclear Fusion, 2021.
[2] D. Haberberger et al., "Measurements of electron density profiles using an angular filter refractometer," Physics of Plasmas, vol. 21, no. 5, p. 056304, 2014.

III-13. Induced Current Due to Electromagnetic Shock Produced by Charge Impact on a Conducting Surface*

Dion Li [a], Patrick Wong [b], David Chernin [c] and Y. Y. Lau [a]

(a) Department of Nuclear Engineering and Radiological Sciences, University of Michigan, Ann Arbor, MI 48109 USA (dionli@umich.edu)
(b) Department of Electrical and Computer Engineering, Michigan State University, East Lansing, MI 48824 USA
(c) Leidos, Inc., Reston, VA 20190 USA

As a charged particle strikes a perfectly conducting plate, an electromagnetic shock is produced at the location of impact [1]. This electromagnetic effect was totally absent in the classical Ramo-Shockley theorem (RS) [2], which has been widely used in radiation detection and measurement and in electronic devices. We compare this electromagnetic shock-induced current with the electrostatic, classical RS [3], using an infinitely long charged rod model moving between two perfectly conducting parallel plates subjected to an RF voltage. In a half RF cycle, the classical RS induced current occurs during charge transit ($t' < 0$, Fig. 1) and the shock-induced current occurs after charge impact on a plate ($t' > 0$). The shock-induced current is insignificant for non-relativistic impact energies but becomes appreciable for mildly relativistic impact velocities. We thus speculate that the electromagnetic shock is negligible in multipactor discharges [4] but could have a considerable effect in magnetically insulated line oscillators (MILOs [5]) and relativistic magnetrons, offering a possible explanation for the characteristically low efficiencies observed in these high power microwave sources, compared with the microwave oven magnetron.

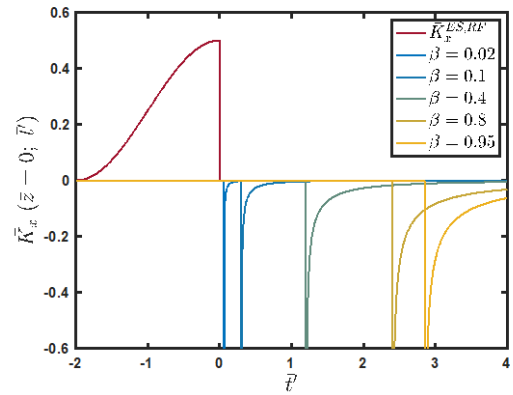

Figure 1 – Time-evolution of the normalized classical, electrostatic (RS) induced current (in red, $t' < 0$), compared with the electromagnetic shock-induced currents of an impacting line charge ($t' > 0$), at five different impact velocities: $\beta =$ 0.02, 0.1, 0.4, 0.8, and 0.95, corresponding to impact energies of, respectively, 0.102, 2.574, 46.54, 340.7, and 1126 keV.

* This work was supported by AFOSR Grants FA9550-18-1-0153, FA9550-18-1-0062, FA9550-20-1-0409, and FA9550-21-1-0367, and by the L3Harris Electron Devices Division.

References

[1] D. Li, D. Chernin, and Y. Y. Lau, "A Relativistic and Electromagnetic Correction to the Ramo–Shockley Theorem," *IEEE Trans. Plasma Sci.*, **49**, 2661 (2021); doi: 10.1109/TPS.2021.3099512.
[2] S. Ramo, *Proc. IRE* **27**, 584 (1939); W. Shockley, *J. Appl. Phys*. **9**, 635 (1938).
[3] D. Li, P. Wong, D. Chernin, and Y. Y. Lau, "Induced Current Due to Electromagnetic Shock Produced by Charge Impact on a Conducting Surface," *IEEE Trans. Plasma Sci.*, (e-published, July 2022). doi: 10.1109/TPS.2022.3187667.
[4] P. Y. Wong, et al., *Phys. Plasmas* **26**, 112114 (2019); doi: 10.1063/1.5125408.
[5] D. A. Packard, et al., *Phys. Plasmas* **28**, 123102 (2021); doi: 10.1063/5.0071455.

III-14. Chemical Mechanical Polishing Rate and Surface Roughness for Single-Crystalline Diamond Substrates*

S M Asaduzzaman and Dr. Timothy Grotjohn

Department of Electrical and Computer Engineering, Michigan State University, Michigan-48824, USA
(asaduzza@msu.edu)

Diamonds are promising candidates in the modern engineering industry. The use of diamonds as a strategic engineering material has long been recognized. Single-Crystalline Diamonds (SCD) developed by Chemical Vapor Deposition (CVD) are excellent candidates for industrial applications, including next-generation electronics, quantum information processing systems, quantum sensors, optical windows, precision machining tools, and diamond bonding to other semiconductors. Diamond surfaces must be exceptionally flat and polished since non-uniform thickness and rough surfaces limit these industrial applications of diamonds. The development of diamond applications in electronics can be greatly improved by precise polishing that produces minimal damage to diamond substrates. Diamonds have been polished using a variety of ways over the years. In terms of material surface finish, Chemical Mechanical Polishing (CMP) process with strong oxidizing slurries to polish CVD diamond films is a promising approach that ensures the diamonds' low surface roughness and high surface quality [1-3].

We have studied the CMP process for polishing diamond substrates/epi-layers. We have looked at quantifying the CMP polishing rate and the uniformity of the polishing across the diamond substrate. We studied the CMP process applied to CVD diamonds grown on the HPHT substrates. This study utilizes High-Pressure High-Temperature (HPHT) diamond samples with a 0-3° degree off-angle from the (001) surface orientation with dimensions of 3.5 x 3.5 mm^2 and larger. Patterns are etched into the diamond surface to study the diamond material polishing rate with the atomic force microscope (AFM) and surface profilometry techniques. The CMP polishing equipment rotates the polishing wheel and sweeps/rotates the sample while using a self-leveling sample holder to maintain contact between the SCD surface and the grooved ceramic polishing wheel. The self-leveling approach helps achieve a repeatable, uniform, and proportionate material removal. With this approach, roughness can be reduced to less than 0.5 nm without aggressively reducing epitaxial layers' thickness or homogeneity. The oxidative CMP slurry mixture consists of potassium permanganate ($KMnO_4$) and boron carbide particles (1-3 µm) with phosphoric acid and DI water. CMP is performed for fixed time intervals with the surface profile of the previously etched structures on the diamond surface measured after each interval to determine CMP removal rates and uniformity. The typical interval time between measurements was 60 minutes. Before and after each hour of CMP operation, microscopic checks, profilometer step scanning, and atomic force microscope (AFM) scans were performed. On the SCD substrate, measurements were performed at multiple locations. The typical CMP removal rates were 95-145 nm/hr.

* The work is supported by Michigan Translational Research and Commercialization (MTRAC).

References

[1] T. Schuelke, T.A. Grotjohn, Diam. Relat. Mater. 32 (2013).
[2] H. Luo, K.M. Ajmal, W. Liu, K. Yamamura, H. Deng, Int. J. Extrem. Manuf. 3 (2021).
[3] Z. Yuan, Z. Jin, Y. Zhang, Q. Wen, J. Manuf. Sci. Eng. Trans. ASME. 135 (2013).

III-15. A Multi-Site Emission Modeling Framework for Porous Electrosprays*

Collin B. Whittaker and Benjamin A. Jorns

University of Michigan Department of Aerospace Engineering (cbwhitt@umich.edu)

A physics-based model predicting the onset of and current emitted from multiple emission sites for porous electrospray emitters is presented. The model predictions take the form of successively higher moments over an emission site distribution function, which may be assigned *ad hoc* or predicated on the porous properties of the emitter substrate. These are then further integrated over the area of the emitter, such that the model can also account for the position-dependent electric field on the emitter surface.

The models are trained via Bayesian inference on experimental data taken by St. Peter *et al* for a single porous electrospray emitter, where the emission current is measured and the total number of emission sites inferred by resolving individual beamlets in the plume of the spray [1]. The trained model is then used to make predictions for a second emitter as a validation case. Finally, the model is used to simulate the emission behavior of an AFET-2, an electrospray thruster consisting of an array of O(500) individual emitters, for which the emitter geometry varies as a result of finite manufacturing tolerance, resulting in emission predicted to be irregular across the array [3].

* This work was supported by a NASA Space Technology Graduate Research Opportunity and by an Early Stage Innovations grant from NASA's Space Technology Research Grants program.

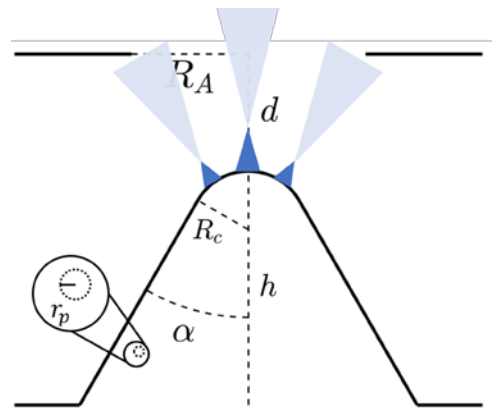

Figure 1 – Schematic depiction of multi-site emission for a porous electrospray emitter with key dimensions labeled.

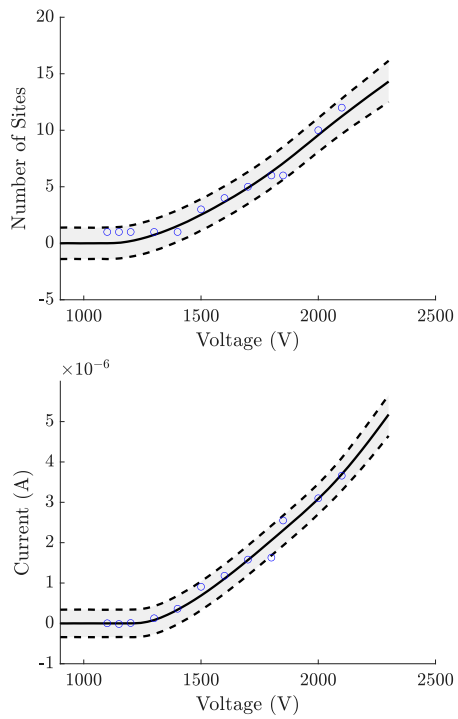

Figure 2 – Predicted (black) number of emission sites (above) and total emission current (below) for a single porous electrospray emitter compared to the training data (blue); the dashed lines are 95% credible intervals [1,2].

References

[1] B. St. Peter et al, Aerospace. **7**, 91 (2020).
[2] C. Whittaker et al, 2022 International Electric Propulsion Conference, IEPC-2022-205, (2022).
[3] Natisin et al. J. Micromech. & Microeng. 30, (2020).

III-16. Model Calibration using an Optimal Experimental Design for Ion Current Density and Ion Energy

Madison G. Allen and Benjamin A. Jorns

University of Michigan, Ann Arbor, MI, 48109 (mgallen@umich.edu)

In recent years, there has been a push for high power Hall Effect Thrusters (HETs) for deep space exploration. One key component necessary for developing high power HETs is testing. Vacuum test facilities are utilized to simulate the low pressures evident of space, but even state of the art facilities do not reach the desired lower pressures by 6 orders of magnitude [1]. It has been found that the difference in pressures result in a discrepancy between the on-orbit Hall thruster performance and plasma behavior and that of ground testing. The focus of this work is the backpressure effect on ion current density of the plasma plume. It is found that the divergence of the plume increases as the backpressure decreases, seen in measurements of ion current density [2]. Low-fidelity models are developed for these plasma properties and extrapolated to space-like pressures to predict on-orbit behavior. These models often require a large amount of data for accurate extrapolation, but an optimal experimental design (OED) with a limited amount of data can be used to calibrate models for the same extrapolation. This is proven with an ion current density and ion energy model that is a function of position and backpressure by identifying the experimental designs with the potential of the model gaining the most information [3]. The method is proven with data from the SPT-100 HET [2] by taking individual optimal designs of pressure and locations for model calibration, as well as batches or groups of locations at a single optimal pressure. By comparing the models calibrated on the full set of data and the limited optimal set of data, model convergence is seen with half of the data.

References

[1] Hofer, R. R., Peterson, P., and Gallimore, A., “Characterizing Vacuum Facility Backpressure Effects on the Performance of a Hall Thruster,” 2001 International Electric Propulsion Conference, 2001.
[2] Diamant, K., Liang, R., and Corey, R., “The Effect of Background Pressure on SPT-100 Hall Thruster Performance,” AIAA/ASME/SAE/ASEE Joint Propulsion Conference, 2014.
[3] Huan, X., and Marzouk, Y. M., “Simulation-based optimal Bayesian experimental design for nonlinear systems,” Journal of Computational Physics, 2013.

List of Participants

Last name	First name	Email	University
Akintola	Ibukunoluwa	iakintol@nd.edu	Notre Dame
Allen	Madison	mgallen@umich.edu	U-M
Angulo Enriquez	Moises	moisesae@umich.edu	U-M
Antoine	André	aantoine@umich.edu	U-M
Asaduzzaman	S M	asaduzza@msu.edu	MSU
Baldinucci	Salvatore	salbal@umich.edu	U-M
Basu	Sankhadeep	basusank@msu.edu	MSU
Bryant	Khalil	kalelb@umich.edu	U-M
Chen	Joe	joech@umich.edu	U-M
Cheng	Zhongyu	zcheng5@nd.edu	Notre Dame
Chuna	Thomas	chunatho@msu.edu	MSU
Dowhan	George	dowhan@umich.edu	U-M
Ernst	Nicholas	npegyf@umich.edu	U-M
Faisal	Md Arifuzzaman	faisalmd@msu.edu	MSU
Herrera-Rodriguez	Cristian	herrer95@msu.edu	MSU
Kabir	Kazi	kazisadman.kabir@rockets.utoledo.edu	UToledo
Kelso	Kwyntero	kkelso@umich.edu	U-M
Kinney	Julian	julkin@umich.edu	U-M
Konina	Kseniia	kseniiak@umich.edu	U-M
Krüger	Florian	fkrueger@umich.edu	U-M
Latham	Joshua	joshla@umich.edu	U-M
Lee	Garam	glee4@nd.edu	Notre Dame
Li	Dion	dionli@umich.edu	U-M
Litch	Evan	elitch@umich.edu	U-M
Marks	Thomas	marksta@umich.edu	U-M
Marshall	Julia	julm@umich.edu	U-M
Mime	Farha Islam	mimefarh@msu.edu	MSU
Narasapura Ramesh	Sandeep	sandeep.narasapuraramesh@rockets.utoledo.edu	UToledo
Nikhar	Tanvi	nikharta@msu.edu	MSU
Papson	Cameron	papsonca@msu.edu	MSU
Paudel	Ayush	paudela1@msu.edu	MSU
Polito	Jordyn	jopolito@umich.edu	U-M
Posos	Taha	pososstah@msu.edu	MSU
Qian	Qian	qqbruce@umich.edu	U-M
Revolinsky	Ryan	revolins@umich.edu	U-M
Roberts	Sarah	rober964@msu.edu	MSU
Roberts	Parker	pjrob@umich.edu	U-M
Sercel	Christopher	csercel@umich.edu	U-M
Springstead	Michael	mispring@umich.edu	U-M
Su	Leanne	leannesu@umich.edu	U-M
Vasey	Gina	vaseygin@msu.edu	MSU
Wadas	Michael	mwadas@umich.edu	U-M
White	Donovan	dejwhite@umich.edu	U-M
Whittaker	Collin	cbwhitt@umich.edu	U-M
Williams	Kelsey	kelseywi@buffalo.edu	SUNY Buffalo
Zhou	Yang	zhouya22@egr.msu.edu	MSU